

Permafrost Mapping through Multi-Source Geospatial Modeling

Mullainathan V H

Sivatmiga T N

BACHELOR OF ENGINEERING

Branch: ROBOTICS AND AUTOMATION



May 2025

**CENTRE FOR ARTIFICIAL INTELLIGENCE AND ROBOTICS
DEFENCE RESEARCH AND DEVELOPMENT ORGANISATION**

Bangalore, India

SYNOPSIS

Permafrost in high-altitude regions causes operational challenges in defense, logistics, and infrastructure planning. The thawing and instability of ground layers can result in road damage, slope movement, and surface deformation. This project focuses on identifying and mapping permafrost probability zones in the Western Himalayas and Russian Arctic using empirical models and satellite data. The objective is to generate permafrost maps at 30-meter resolution using environmental inputs such as temperature, vegetation, soil, and elevation. The work includes computing TTOP (Temperature at the Top of Permafrost), MAGT (Mean Annual Ground Temperature), and ALT (Active Layer Thickness), and using these to classify zones based on likelihood of permafrost presence.

The process begins with satellite data collection and preprocessing using Google Earth Engine (GEE). Datasets include MODIS LST, NDVI, NDSI, ERA5 temperature, and SRTM DEM, covering the years 2020 to 2023. Each raster is filtered, clipped to the study area, and resampled to 30 meters. Terrain indices like slope and aspect are derived. Freezing Degree Days (FDD) and Thawing Degree Days (TDD) are computed using lapse-corrected ERA5 data. A local Python script then applies three separate empirical models: TTOP is estimated from MAAT, soil conductivity, and surface n-factors; MAGT is modeled using a linear combination of terrain and climate layers; and ALT is calculated using Stefan's formula. These outputs are normalized and combined into a permafrost probability index, which is then classified into high, moderate, and low categories.

The final maps show the extent and distribution of probable permafrost zones across the selected regions. In the Himalayas, high-altitude locations above 3500 m show higher probability values. In the Russian Arctic, near-continuous permafrost appears across the region. Output layers including MAGT, ALT, and TTOP were validated using reference borehole datasets and known geocoded observations. Comparison metrics such as RMSE, MAE, Pearson correlation, F1-score, and Intersection over Union (IoU) were used. Maps were generated with location markers, elevation profiles, and classification overlays to support visual interpretation. This model helps identify terrain areas with permafrost conditions and can be applied for further analysis in environmental monitoring and logistics.

CONTENTS

CHAPTER	Page No.
Acknowledgement	(i)
Synopsis.....	(ii)
List of Figures	(iii)
List of Tables	(iv)
List of Abbreviations	(v)
1 INTRODUCTION.....	1
1.1 Problem Statement	1
1.2 Motivation	1
1.3 Background	3
1.4 Objectives of the Project	9
1.5 Scope of the Project	10
1.6 Organization of the Report	11
2 LITERATURE REVIEW.....	12
2.1 Literature Reviewed	12
2.2 Overview Of Permafrost Studies	15
2.3 Empirical And Semi-Empirical Models	16
2.4 Remote Sensing for Cryosphere Monitoring	16
2.5 Terrain Influence	17
2.6 Soil and Vegetation Influence	17
2.7 Indian context and Defense Relevance	17
2.8 Identified Gaps and Research Direction	18
3 STUDY AREA AND DATA SOURCES.....	19
3.1 Geopolitical Significance	19
3.2 Terrain and Climate Profile	21
3.3 Ground Validation and In-situ Limitations	24

3.4	Raster and Reanalysis Datasets Used	25
3.5	Platforms and Tools	27
4	ARCHITECTURE AND METHODOLOGY.....	29
4.1	Overall System Architecture	29
4.2	Methodology	31
4.3	Terrain Variable Generation	34
4.4	Climate Index Processing	35
4.5	Vegetation and Snow Cover Indices	36
4.6	Soil Parameter Integration	37
4.7	Empirical Model Computation	38
4.8	Composite Permafrost Probability Map	39
4.9	High-Confidence Permafrost Mask	40
4.10	Overlay Of Names and Terrain Labels	40
5	IMPLEMENTATION	41
5.1	GEE for Raster Generation	41
5.2	Permafrost modelling	43
5.3	Visualization Pipeline	45
5.4	Indicators and their Meaning	46
6	RESULTS AND EVALUATION.....	49
6.1	Raster Preprocessing and Alignment	49
6.2	Permafrost Modelling	55
6.3	Zonal Classification	59
6.4	Map Verification with Ground Truth	60
7	CONCLUSION.....	65
7.1	Summary of Work Done	65
7.2	Key Observations	66
7.3	Limitations of Current Study	66
7.4	Climate Monitoring and Defense Synergy	68
7.5	Final Remarks	68
	BIBLIOGRAPHY	69
	APPENDIX	71

CHAPTER 1

INTRODUCTION

This chapter provides the foundational context for the report, beginning with a clear articulation of the problem addressed being navigational challenges for autonomous vehicles in permafrost-affected high-altitude regions. The chapter explains the motivation behind selecting this research area, highlighting its relevance to defense operations, data gaps, and the potential of satellite-based mapping. It then offers essential background on permafrost covering definitions, classifications, structure, and key indicators along with established methods for its survey and mapping. The chapter further outlines the unique challenges posed to autonomous systems by permafrost terrain, and specifies the objectives and operational scope of the study. Finally, it presents the structure of the report to guide through the subsequent chapters.

1.1 PROBLEM STATEMENT

Autonomous tanker vehicles operating in varying terrains like the Western Himalayas face navigational risks due to undetected or degrading permafrost, which compromises terrain stability. The absence of high-resolution, localized permafrost data hampers reliable path planning and terrain-aware autonomy. This project aims to generate 30-meter resolution permafrost probability maps using publicly available satellite data sources. The maps are developed by combining thermal models, terrain derivatives, and soil parameters, which can be further integrated as no-go regions into the autonomous vehicle's path planning algorithm to improve safety, efficiency, and mission success in high-altitude operations.

1.2 MOTIVATION

Outlined below are the primary motivations that highlight the importance of this work and establish the necessity for a focused project in this area:

1. Relevance in Defense Operations

- The Armed Forces and logistics units frequently operate in permafrost-prone high-altitude regions and strategically significant zones such as Siachen Glacier, Drass Valley, Depsang Plains, Changthang Plateau, Daulat Beg Oldie (DBO), Galwan Valley, and Pangong Tso in Ladakh; Batalik, Mushkoh, and Kargil sectors in Jammu & Kashmir. Spiti Valley, Bara-lacha La, and Rohtang Pass in Himachal Pradesh; Niti and Mana Passes in Uttarakhand; Lachen, Lachung, and Gurudongmar Lake region in North Sikkim; Forward posts near Tawang, Walong, and the Gorichen range in Arunachal Pradesh. These locations are typically situated at elevations between 3,500 to 6,000 meters, where seasonal freeze-thaw cycles and the presence of ice-rich soil increase the risk of permafrost-related terrain deformation. Many of these regions lie along or near the Line of Actual Control (LAC) and Line of Control (LoC). The Indian Army, Indo-Tibetan Border Police (ITBP), and Border Roads Organisation (BRO) maintain a year-round presence in these areas to support logistics, infrastructure, and security operations.
- Slope instability, road subsidence, foundation failure, and localized flooding due to thawing ground ice are common hazards in such zones, all of which directly impact troop mobility, supply chain reliability, and autonomous vehicle performance.
- Without reliable terrain stability data, these systems risk becoming immobilized or damaged, which could compromise both logistical efficiency and mission safety and so autonomous tanker vehicles, designed to reduce human risk in harsh terrains, must avoid such geotechnically unstable zones to function effectively.

2. Lack of High-Resolution Permafrost Data

- Existing global permafrost datasets (e.g., Permafrost Zonation Index, Circum-Arctic Map) are too coarse (1 km or more) and not calibrated for Indian terrains.
- No open-access, high-resolution (30 m) permafrost maps are available for Indian zones, creating a critical data gap for defense applications.

3. Use of Public Satellite Data for Cost-Effective Mapping

- Satellite imagery from MODIS, Landsat, Bhuvan, and ERA5 climate reanalysis is freely available, making it feasible to generate localized maps at scale.
- Platforms like Google Earth Engine (GEE) enable processing large raster datasets with ease, eliminating the need for expensive proprietary software or high-performance computing resources.

4. Relevance to Autonomous Navigation

- In autonomous mobility systems, terrain-aware planning is essential. Just elevation and slope are not sufficient, permafrost zones introduce additional instability risks not captured by topography alone.
- To integrate permafrost zones as dynamic terrain constraints (no-go areas) in the future that helps enhance the decision-making logic of autonomous systems and prevents unsafe route generation.

5. Climate Monitoring

- As permafrost is a climate-sensitive indicator, its mapping helps monitor long-term trends in regional warming and associated terrain transformations.
- This aligns with national and global efforts to track climate vulnerabilities in ecologically fragile high-altitude zones.

1.3 BACKGROUND

1.3.1 Permafrost overview

Permafrost refers to any ground composed of soil, sediment, rock, or organic material that has remained at or below 0°C (freezing point of water) for at least two consecutive years. The term “permafrost” does not mean that the ground is always covered with snow or ice. Rather, it defines a thermal condition of the subsurface. Even dry, rocky ground can be classified as permafrost if it remains frozen over time and it is found in two primary environmental settings:

1. Polar regions, such as Siberia, Alaska, and the Canadian Arctic.
2. High-altitude regions, such as the Tibetan Plateau, the Andes, and the Himalayas.

Permafrost covers nearly 24% of the exposed land in the Northern Hemisphere. Its depth can vary from just a few meters to over 1,500 meters in some Arctic zones. It is not uniform and it may contain layers of pure ice, mixed soils, rocks, or frozen peat.

1.3.2 Permafrost Structure

Permafrost is not a single monolithic layer as seen in figure 1.1. It has a distinct vertical structure that comprises of the 4 predominant layers as follows:

- Active Layer: This is the top layer of ground above the permafrost that thaws during summer and refreezes in winter. Its thickness can vary from 20 centimeters to several meters, depending on local climate, vegetation, and snow insulation. It is crucial because most biological activity and surface processes happen within this layer.

- Permafrost Table: The top boundary of the permanently frozen ground beneath the active layer.
- Perennially Frozen Ground: Below the permafrost table is the zone that remains completely frozen year-round. It contains a combination of mineral particles, organic material, water (in the form of ice), and gases like methane.
- Taliks: These are unfrozen patches that exist above, within, or below the permafrost. They may be caused by bodies of water (which retain heat), geothermal energy, or insulation from thick snow cover.

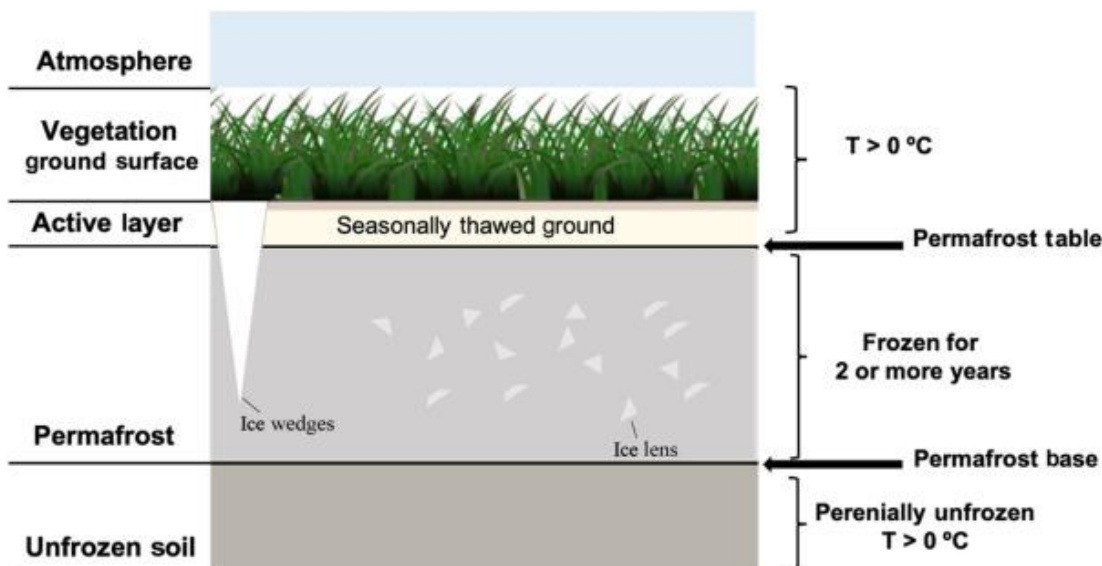


Fig 1.1 Permafrost layers

1.3.3 Permafrost Classification

Permafrost is generally categorized based on its spatial extent and is classified as the following types:

- Continuous Permafrost: Covers over 90% of the landscape in very cold regions. Found in the Arctic and at very high altitudes.
- Discontinuous Permafrost: Covers between 50–90% of an area, often with warm microclimates that interrupt the frozen ground.
- Sporadic Permafrost: Exists in less than 50% of an area, typically in sheltered zones or north-facing slopes.
- Isolated Patches: These are small, local spots of frozen ground in otherwise unfrozen terrain.

1.3.4 Significant Implications of permafrost

- Terrain Stability: Ice within permafrost acts like cement. When it melts, the ground can collapse, leading to slope failures, landslides, or subsidence. This affects roads, buildings, pipelines, and vehicles.
- Hydrology: Permafrost impedes water drainage. In permafrost regions, rainfall often stays near the surface, forming wetlands, bogs, or thermokarst lakes (formed due to ground ice thawing and collapsing).
- Carbon Storage: Permafrost soils lock away vast amounts of carbon over 1,600 gigatonnes, nearly twice the carbon currently in the atmosphere. As the ground thaws, organic material decomposes and releases greenhouse gases like carbon dioxide and methane, amplifying climate change.
- Ecosystem Support: Permafrost supports unique ecosystems like tundra and alpine meadows. Thawing permafrost can drastically alter the distribution of species and habitat quality.

1.3.5 Common Permafrost Indicators

Indicator	Description
LST (Land Surface Temperature)	Measures surface freeze/thaw conditions.
NDVI (Normalized Difference Vegetation Index)	Indicates vegetation cover and ground insulation.
NDSI (Normalized Difference Snow Index)	Detects snow cover and its thermal insulation effect.
MAAT (Mean Annual Air Temperature)	Long-term average air temperature.
MAGT (Mean Annual Ground Temperature)	Average annual ground temperature at depth.
TTOP (Temperature at Top of Permafrost)	Empirically estimated permafrost surface temperature.
FDD (Freezing Degree Days)	Cumulative cold exposure below 0°C.
TDD (Thawing Degree Days)	Cumulative heat exposure above 0°C.
ALT (Active Layer Thickness)	Depth of seasonal thaw above the permafrost layer.
Slope	Influences water drainage, snow retention, and heat transfer.
Aspect	Directional orientation influencing solar exposure.

Elevation (from DEMs)	High elevations are colder and more likely to preserve permafrost.
Soil Texture	Composition (sand, silt, clay) affects thermal and hydrological behavior.
Bulk Density	Mass per unit volume; affects thermal conductivity.
Snow Depth and Duration	Longer snow cover delays ground freezing.
Vegetation Type and Density	Dense vegetation alters freeze/thaw dynamics.
Ground Ice Content	Higher ice content increases thaw-induced deformation risk.
Surface Water Presence	Water bodies can slow freezing or cause unfrozen taliks.

1.3.6 Permafrost Survey Methods

Mapping permafrost involves determining where the ground stays frozen year-round and how its thermal and physical properties change across space and time. Since direct observation (digging or drilling) is expensive and often impossible in remote or hazardous regions, scientists use a combination of ground-based measurements, remote sensing technologies, and computational models. Below is a list of predominantly known categories and methods used for permafrost mapping:

1. Ground-based Methods

These are on-site techniques that provide highly accurate and detailed local information. They are indispensable for validation and long-term monitoring but are limited in spatial coverage.

- **Boreholes and Thermistor Chains:** Boreholes are drilled into the ground and equipped with thermistors (temperature sensors) placed at various depths to continuously monitor ground temperatures. This helps determine the depth of the active layer (seasonally thawed) and locate the top of the permafrost.
- **Electrical Resistivity Tomography (ERT):** This technique sends electrical currents through the ground. Frozen ground, especially if ice-rich, has high resistivity, whereas thawed or water-saturated soil conducts electricity more easily. ERT helps visualize subsurface freeze/thaw boundaries.

- Ground Penetrating Radar (GPR): GPR uses high-frequency radar pulses to detect changes in underground materials. It's useful for identifying ice lenses, thaw boundaries, and taliks (unfrozen zones in permafrost).
- Seismic Refraction Surveys: Seismic waves travel faster through frozen, compacted ground than thawed, loose soil. By measuring the speed of these waves, scientists can infer permafrost depth and structure.
- Borehole Logging (Geophysical and Geochemical): Boreholes are also used to log other properties like soil conductivity, density, and the presence of gas or moisture—all of which help confirm permafrost conditions.
- Soil Gas Sampling (CH_4 , CO_2): In thawing permafrost, microbial decomposition releases greenhouse gases. Measuring methane and carbon dioxide levels can indicate permafrost degradation.
- Active Layer Thickness Monitoring (CALM Program): The Circumpolar Active Layer Monitoring (CALM) network tracks the thickness of the seasonal thaw layer across time using stakes, frost tubes, or temperature probes.
- Cryostratigraphy and Core Analysis: Frozen soil cores extracted from drilling are examined in labs for ice content, cryostructure (pattern of ice within soil), grain size, and organic carbon.

2. Remote Sensing Techniques

These techniques use satellites or airborne sensors to monitor large or inaccessible areas, providing regular data on temperature, vegetation, terrain, and soil moisture. They are ideal for mapping permafrost at continental to regional scales.

- Land Surface Temperature (LST): Satellites like MODIS, Landsat, and ECOSTRESS monitor surface temperature over time. Long-term averages help estimate subsurface temperatures related to permafrost stability.
- Normalized Difference Vegetation Index (NDVI): This spectral index indicates the presence and health of vegetation. Tundra vegetation like mosses and lichens are often linked with permafrost zones.
- Normalized Difference Snow Index (NDSI): NDSI measures snow cover from optical satellite data. Snow acts as an insulator and affects ground freezing and thawing patterns.
- Digital Elevation Models (DEM): Elevation, slope, and aspect influence solar radiation and insulation. Permafrost is more common on high, north-facing slopes.

- Synthetic Aperture Radar (SAR): SAR sensors can see through clouds and operate at night. They detect surface roughness, snow accumulation, and frozen soil conditions.
- Interferometric SAR (InSAR): This technique measures millimeter-level ground movement over time. It's used to detect surface subsidence from thawing permafrost.
- Backscatter Intensity (from Sentinel-1): Radar backscatter reflects differences in surface moisture and dielectric properties, which vary between frozen and thawed soils.
- Thermal Inertia Analysis: By tracking how quickly surfaces heat up or cool down, scientists can distinguish between water, snow, dry ground, and frozen soil.
- Vegetation Functional Type Mapping: Classification of land cover types (tundra, bog, wetland) helps infer the likelihood of permafrost beneath based on ecological correlations.
- LiDAR (Light Detection and Ranging): Airborne laser scanning creates high-resolution terrain maps. Changes in microtopography (like frost heave or thermokarst) reveal permafrost dynamics.
- UAV-Based Sensing: Drones equipped with thermal cameras, multispectral sensors, or mini-LiDAR systems are used for small-area, high-detail permafrost studies.
- Passive Microwave Sensors (e.g., SMOS, AMSR-E): These sensors detect soil freeze/thaw states and moisture from space, useful for broad seasonal monitoring.
- Photogrammetry (Structure-from-Motion): Aerial or drone-based photographs processed into 3D models to detect small terrain changes associated with thaw.

3. Empirical and Analytical Models

Models use climatic, soil, terrain, and vegetation data to estimate permafrost presence and behavior. They range from simple equations to advanced simulation tools.

- TTOP (Temperature at the Top of Permafrost): This semi-empirical model estimates the ground temperature just above permafrost using air temperature, snow/vegetation n-factors, and soil thermal properties.
- MAGT (Mean Annual Ground Temperature): Estimates long-term average ground temperature at depth, often inferred using terrain and climate indices.
- ALT (Active Layer Thickness): Calculated using Stefan's equation, which uses Freezing Degree Days (FDD), latent heat of fusion, soil bulk density, and conductivity.
- Permafrost Zonation Index (PZI): A composite index used in global maps (e.g., Circum-Arctic Map) to classify regions into permafrost probability zones.

- CryoGrid Model: A 1D/2D physical model simulating energy and water fluxes through ground layers, including phase changes in permafrost.
- GEOTop, CoupModel, and PFLOTRAN: Full land-surface models that simulate freeze/thaw cycles, water flow, and heat transport.
- Machine Learning Models (Random Forest, SVM, Neural Networks): Trained on satellite and borehole data to classify terrain as permafrost or not.
- Bayesian and Probabilistic Models: Combine uncertain parameters (e.g., MAAT, snow depth, NDVI) to estimate the likelihood of permafrost occurrence.

1.4 OBJECTIVES OF THE PROJECT

1. Permafrost Probability Mapping

- To generate 30-meter resolution permafrost probability maps over selected high-altitude regions of the Western Himalayas, including areas above 3,500 m elevation where permafrost conditions are expected.
- To delineate permafrost presence using a multi-criteria approach combining thermal, terrain, vegetation, and snow indices into a composite permafrost probability score.

2. Empirical Model Computation

- To compute TTOP (Temperature at the Top of Permafrost) using MAAT, vegetation (n-factors), and soil thermal properties.
- To compute MAGT (Mean Annual Ground Temperature) through a regression model incorporating land surface temperature (MODIS), NDVI, DEM, and slope.
- To compute ALT (Active Layer Thickness) using Stefan's Law with Freezing Degree Days (FDD), bulk density, and thermal conductivity.
- To apply resampling, raster alignment, and normalization techniques to ensure consistent spatial resolution and format across all datasets.

3. Thematic Classification of Permafrost Zones

- To classify modeled permafrost probability into high, moderate, and low-confidence zones using empirical thresholds.
- To visually validate the permafrost zones using reference datasets.

4. Geospatial Analysis Pipeline Implementation

- To use Google Earth Engine (GEE) for large-scale raster preprocessing including MODIS LST averaging, NDVI and NDSI extraction, and ERA5-derived FDD/TDD computation.

- To develop a Python-based modeling framework for permafrost estimation and visualization, leveraging rasterio, NumPy, and matplotlib.

5. Raster Data Management and Visualization

- To generate and export high-resolution GeoTIFF maps of individual model outputs of TTOP, MAGT, ALT, a composite permafrost probability, a classified permafrost extent
- To produce annotated visualizations overlaying place names, elevation contours, and slope profiles for intuitive understanding by military and scientific users.

6. Future Enhancement

- To provide actionable terrain intelligence for defense logistics and troop mobility, particularly in regions prone to seasonal thaw-induced hazards such as road collapse or foundation failure.
- To contribute to climate-sensitive terrain modeling by tracking changes in thermal parameters related to permafrost degradation in fragile ecological zones.
- To establish a scalable methodology that can be replicated for other regions like Russia, Central Asia, or Antarctica.

1.5 SCOPE OF THE PROJECT

This study is scoped to develop a satellite-based, non-intrusive framework for estimating and classifying permafrost zones in data-scarce high-altitude environments, specifically for operational defense and mobility applications. It delineates the technical, spatial, and methodological boundaries of the work and clarifies the tools and assumptions applied throughout the modeling process.

1. Geographic and Temporal Coverage

- Western Himalayas (India): 75.5°E to 80.5°E longitude and 28.5°N to 36.5°N latitude.
- Yamal region (Russia): 75.5°E to 80.5°E longitude and 67.0°N to 71.0°N latitude.

All inputs are limited to the 2020–2023 period, ensuring temporal consistency across LST, NDVI, NDSI, and ERA5-based thermal indices.

2. Data Inclusion and Standardization

The scope is restricted to freely available satellite and reanalysis datasets, resampled and aligned to a 30-meter resolution. These include:

- MODIS (LST, NDVI)
- Landsat/Sentinel (NDSI)

- SRTM DEM (terrain derivatives)
- ERA5-Land (temperature for FDD/TDD)
- SoilGrids (bulk density, clay, texture, coarse fragments)

All raster products are spatially harmonized using Python tools like rasterio and scikit-image to create a seamless geospatial input stack.

3. Toolchain and Implementation Environment

- Google Earth Engine (GEE): For initial preprocessing of MODIS, Landsat, and ERA5 products.
- Python environment: For empirical modeling, normalization, and map generation.
- QGIS/Matplotlib: For visual overlays and cartographic rendering.

4. Modeling Assumptions and Boundaries

- Only empirical and semi-empirical models are used. These are parameterized from literature, not trained from ground data.
- Vegetation and snow cover are treated as surface modifiers (n-factors) without time-series dynamics or seasonal feedback modeling.
- Soil thermal properties are derived solely from bulk density and clay content, with no calibration from in-situ samples or lab tests.
- No subsurface measurements (e.g., ERT, GPR) are considered in this phase due to access limitations.

5. Output Constraints

- Individual GeoTIFFs: TTOP, MAGT, ALT
- Composite raster: Permafrost probability score
- Categorical classification: Binary and trinary masks
- Visual maps with annotated strategic locations

1.6 ORGANIZATION OF THE REPORT

The report is organized into the following six chapters:

- Chapter 1: Introduces the problem, context, motivation, and study objectives
- Chapter 2: Reviews relevant literature and modeling techniques
- Chapter 3: Describes the study region, input datasets, and tools used
- Chapter 4: Outlines the methodology including preprocessing and model computation

- Chapter 5: Details the implementation pipeline in GEE and Python
- Chapter 6: Presents output maps, analysis, and implications for defense
- Chapter 7: Concludes with key findings and outlines future improvements
- Chapter 8: Lists references used
- Appendices: Provide code, metadata, ratings tables, and additional maps

CHAPTER 2

LITERATURE REVIEW

This chapter reviews existing research, methodologies, and datasets relevant to permafrost mapping, empirical modeling, and their application in high-altitude autonomous mobility. It begins by summarizing key international and Indian studies that have shaped our current understanding of permafrost distribution, thermal modeling, and monitoring techniques. The chapter also examines advances in remote sensing platforms, empirical and semi-empirical models (such as TTOP, MAGT, and ALT), and the role of terrain, soil, and vegetation variables in permafrost assessment. Special attention is given to the Indian context and defense relevance, highlighting gaps in current research, limitations of available datasets, and the need for integrated, high-resolution permafrost mapping in operational planning. The survey concludes by identifying critical research gaps and framing the direction for the present study.

2.1 LITERATURE REVIEWED

2.1.1 Modelling Permafrost Distribution in Western Himalaya Using Remote Sensing and Field Observations (Khan et al., 2021)

This study maps permafrost distribution in the Western Himalaya using satellite data and field measurements. The authors used temperature, solar radiation, slope, aspect, and land cover data to estimate permafrost extent at a 30 m grid scale. They concluded that approximately 25% of the region contains continuous permafrost, 35% has discontinuous permafrost, and 39% has no permafrost. From 2002 to 2020, the total permafrost area declined by around 3% due to rising temperatures. Field validation confirmed the satellite-based results. However, the method had limitations in areas with dense vegetation or deep shadows. [1]

2.1.2 PIC v1.3: Comprehensive R Package for Computing Permafrost Indices over the Qinghai–Tibet Plateau (Luo et al., 2021)

This paper introduces PIC v1.3, an R package designed to calculate 16 permafrost indices using weather and atmospheric forcing data, including MAAT, TTOP, FDD, and ALT. The model was applied over the Qinghai–Tibet Plateau to detect temporal changes in permafrost. Results confirmed regional thawing trends consistent with earlier findings. While the tool is powerful, it depends heavily on the availability of high-quality input data and lacks in-situ field validation. [2]

2.1.3 Circum-Arctic Map of Permafrost and Ground Ice Conditions (Brown et al., 1997)

This foundational study introduced a global permafrost classification scheme dividing the Arctic into continuous, discontinuous, sporadic, and isolated zones. It remains a key reference for global-scale modeling and historical comparison of permafrost extent. [3]

2.1.4 Climate and the Limits of Permafrost: A Zonal Analysis (Smith and Riseborough, 2002)

This study introduced the TTOP model, which calculates the temperature at the top of permafrost using MAAT, snow cover, and vegetation factors. It provided a zonal framework that is still used in empirical permafrost modeling. [4]

2.1.5 Spatial and Temporal Variability in Active Layer Thickness (Zhang et al., 2005)

The authors used long-term Russian borehole datasets to analyze ALT variability in the Arctic. Their work demonstrated how ALT is affected by snow depth, vegetation, and temperature. This study emphasized the need for long-term monitoring in permafrost research. [5]

2.1.6 Google Earth Engine: Planetary-Scale Geospatial Analysis (Gorelick et al., 2017)

This paper established GEE as a powerful platform for remote sensing applications, including permafrost mapping. GEE supports MODIS, Landsat, Sentinel, and elevation datasets—making it ideal for integrated, cloud-based cryosphere modeling. [6]

2.1.7 Remote Sensing of Permafrost and frozen ground (Westermann et al., 2015)

This work showed how combining MODIS LST with NDVI can estimate ground thermal conditions. The model produced surface temperature-based predictions of MAGT, forming the basis for data-driven permafrost monitoring. [7]

2.1.8 Characteristics of the Recent Warming of Permafrost in Alaska (Osterkamp, 2007)

Using multi-decadal borehole data, this study confirmed rapid permafrost warming in Alaska. It served as empirical evidence to validate satellite-derived and model-based permafrost predictions. [8]

2.1.9 National Remote Sensing Centre: Bhuvan Geoportal (ISRO, 2025)

ISRO's Bhuvan platform provides terrain, snow, and vegetation layers useful for permafrost analysis. Although not dedicated to permafrost, Bhuvan data can support permafrost mapping in India when integrated with thermal and terrain models. [9]

2.1.10 Studies on Permafrost in the Western Himalayas (WIHG, 2020)

This technical report outlines permafrost-related research efforts in Ladakh and surrounding areas. It recommends establishing dedicated monitoring stations and integrating remote sensing tools for national-scale assessment. [10]

2.1.11 Snow and Permafrost Studies in Ladakh Using Remote Sensing (Negi et al., 2021)

The study used MODIS and Landsat imagery to identify permafrost-prone areas in Ladakh, correlating snow persistence with elevation and slope. It demonstrated the utility of NDSI in identifying frost-affected terrain. [11]

2.1.12 The ERA5 Global Reanalysis Dataset (Hersbach et al., 2020)

ERA5 offers hourly reanalysis data that supports modeling of FDD, TDD, and MAAT. It is widely used in permafrost thermal simulations but requires terrain-aware corrections for accuracy in mountainous zones. [12]

2.2 OVERVIEW OF PERMAFROST STUDIES

Global efforts in permafrost mapping and monitoring have been led by institutions such as the International Permafrost Association (IPA), USGS, and national cryospheric research agencies. Brown et al. [3] developed the Circum-Arctic Permafrost Map, which remains the foundational dataset for modeling and classification. Studies by Romanovsky et al. and Schuur et al. have extensively analyzed permafrost feedback to climate change and carbon cycling. In Russia and Alaska, field-based monitoring networks measure long-term permafrost trends using boreholes and surface data.

Indian studies have been comparatively limited. Research institutions such as WIHG have reported localized observations in Ladakh and the Western Himalayas. Negi et al. [11] employed satellite datasets for identifying snow and frozen soil characteristics, while Khan et al. [1] attempted empirical modeling at a 30-meter scale. However, due to limited ground validation and absence of continuous monitoring stations, most Indian models remain uncalibrated and coarse in spatial resolution.

2.3 EMPIRICAL AND SEMI-EMPIRICAL MODELS

TTOP (Smith and Riesborough, 2002) calculates temperature at the top of permafrost using a simplified heat transfer equation involving n-factors. It accounts for the influence of vegetation (n_f) and snow insulation (n_t), modifying the mean annual air temperature (MAAT) to infer subsurface temperatures. MAGT represents the average temperature of the ground at a depth where annual fluctuations become negligible, usually approximated by remote sensing-derived LST values adjusted for surface modifiers.

ALT is modeled using Stefan's equation, which relates thaw depth to FDD, soil thermal conductivity, and density. Jafarov et al. [7] and Luo et al. [2] demonstrated applications of these models in Alaska and Tibet using weather datasets and remote sensing. Although empirical models offer computational efficiency and require limited input data, their generalizability is constrained by lack of calibration and soil parameter variability.

2.4 REMOTE SENSING FOR CRYOSPHERE MONITORING

MODIS offers global LST and vegetation indices (NDVI) at daily to bi-weekly resolution. Westermann et al. [6] combined MODIS LST with NDVI to estimate surface thermal regimes and identify permafrost zones. Landsat provides higher spatial resolution (30 m) data suitable for topographic and vegetation monitoring, although its 16-day revisit period limits temporal analysis.

Sentinel-1 and Sentinel-2 support high-resolution SAR and optical imagery respectively. Liu et al. and other researchers have demonstrated the use of Sentinel-1 InSAR for detecting thaw-induced ground deformation. ERA5, developed by ECMWF, offers hourly reanalysis data of temperature, pressure, soil moisture, and wind. ERA5-derived FDD and TDD are widely used in ALT computation (Hersbach et al. [12]). However, the downscaling of ERA5 data to rugged terrain requires lapse rate corrections and fine-tuning for terrain heterogeneity.

2.5 TERRAIN INFLUENCE

DEM-derived terrain features significantly influence permafrost occurrence. Elevation affects air temperature through the lapse rate, while slope and aspect determine solar exposure. North-facing slopes in the Northern Hemisphere retain more snow, leading to cooler and more stable thermal conditions (Lewkowicz and Bonniventure [11]). Cao et al. [12] observed that steeper slopes promote drainage and sunlight exposure, reducing permafrost stability.

In high mountain regions, permafrost typically starts above 3,500 meters elevation, but thresholds vary based on microtopographic features, shading, wind-driven snow distribution, and vegetation cover.

2.6 SOIL AND VEGETATION INFLUENCE

Soil composition plays a critical role in ground heat transfer. High clay content, moisture retention, and bulk density result in stronger freeze-thaw buffering. Hugelius et al. [14] developed global soil thermal maps which are now part of SoilGrids.

Vegetation affects surface albedo, evapotranspiration, and insulation. NDVI is a widely used proxy to classify vegetation cover and indirectly infer insulation characteristics. Zhang and Barry [16] correlated NDVI with MAGT, while NDSI from Landsat is used to monitor snow persistence. Persistent snow cover, as observed via high NDSI values, delays thawing and contributes to active layer thinning.

2.7 INDIAN CONTEXT AND DEFENSE RELEVANCE

Permafrost conditions exist in Ladakh, Himachal Pradesh, North Sikkim, and parts of Uttarakhand. These zones coincide with Indian Armed Forces' operational areas. Permafrost-induced instability has impacted roads, fuel storage, helipads, and communication posts. Despite this, India lacks a centralized permafrost monitoring or forecasting system.

Current research by WIHG involves remote sensing analysis and short-term field visits. However, absence of permanent borehole stations limits long-term monitoring. Bhuvan geoportal [9] by ISRO provides valuable remote sensing data layers, but integration with permafrost modeling is yet to be formalized.

Given increasing use of autonomous systems in high-altitude zones, integrating permafrost layers into mobility planning becomes strategically vital. Terrain-aware planning

algorithms (e.g., A*, Hybrid A*) can avoid geotechnically unstable zones if fed with permafrost probability layers.

2.8 IDENTIFIED GAPS AND RESEARCH DIRECTION

- Most global permafrost datasets (e.g., Brown et al., IPA map) exclude Himalayan terrain or use coarse grid resolution not suitable for local application.
- Lack of ground-based data for model calibration and validation in India severely limits confidence in results.
- Indian studies lack integration of snow dynamics (from NDSI), ERA5-derived climate indices (FDD/TDD), and high-resolution DEMs into a unified framework.
- Use of SAR (InSAR, backscatter intensity) for monitoring seasonal thaw subsidence remains underexplored.
- There is no dedicated Indian platform that integrates remote sensing, empirical modeling, and in-situ observation for permafrost mapping.
- Climate-driven permafrost degradation has not been comprehensively linked to defense mobility constraints in operational terrain models.

CHAPTER 3

STUDY AREA AND DATA SOURCES

This chapter outlines the overall system architecture and design strategy for the terrain-constrained A* path planner. It describes the modular structure of the system, including terrain data preprocessing, the core A* planning logic, and visualization components. Key processes such as DEM and slope map generation, GO/NO-GO area masking, cost function design, and heuristic formulation are detailed. The chapter also introduces enhancements like morphological dilation, PRM integration, and support for advanced A* variants such as Theta*. These components collectively form a scalable and adaptable framework for realistic path planning in unstructured terrains.

3.1 GEOPOLITICAL SIGNIFICANCE

This research is conducted over two permafrost-affected regions that represent significantly different geophysical, climatic, and strategic characteristics: **the Western Himalayas (India)** and the **Yamal Peninsula (Russia)**. While the former is a high-altitude, tectonically active region with military relevance, the latter represents a polar lowland terrain influenced by Arctic climatology and cryogenic ground structures. By modeling both regions with a consistent pipeline, the study compares distinct permafrost types—alpine vs. arctic—and lays groundwork for scalable mapping across geopolitical terrains.

3.1.1 Western Himalayas, India

The Western Himalayas encompass the union territory of Ladakh and parts of Himachal Pradesh, Uttarakhand, and North Sikkim. The area lies between latitudes **28.5°N to 36.5°N** and longitudes **75.5°E to 80.5°E**, covering a spatially complex zone characterized by abrupt elevation gradients, glaciated valleys, and sparse vegetation as seen in figure 3.1.

This region is critically important from a defense logistics and national security standpoint. It hosts:

- High-altitude military bases and logistic depots
- Strategic roads like the Darbuk–Shyok–DBO route
- Forward posts in snow-bound sectors with limited access

The region is also directly adjacent to international boundaries. In the north and east, the Line of Actual Control (LAC) demarcates a disputed border with China, passing through areas like Depsang Plains, Galwan Valley, and Pangong Tso. In the west, the Line of Control (LoC) interfaces with Pakistan-administered territory, adding another dimension of geopolitical sensitivity.

Due to these factors, the terrain is under constant use by personnel, heavy vehicles, and, increasingly, by autonomous ground systems. However, these operational demands occur in zones where ice-rich permafrost is present, introducing risks of terrain instability such as thaw settlement, road subsidence, and slope collapse. Mapping permafrost in this context provides direct value to national defense and terrain-based risk mitigation.

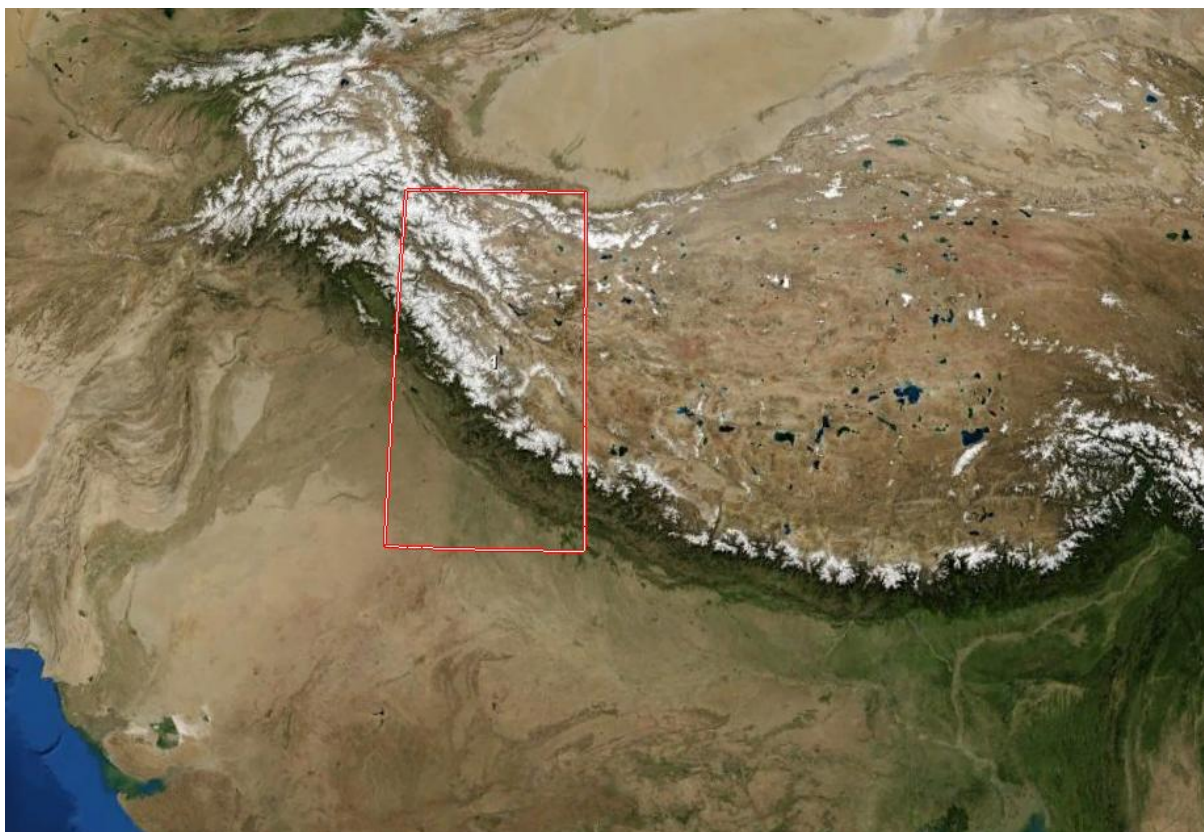


Fig 3.1 ROI Western Himilayas

3.1.2 Yamal Peninsula, Russia

To validate the model's global applicability and examine its performance in a contrasting permafrost environment, the study also includes the Yamal Peninsula located in northwest Siberia, between **67.0°N and 71.0°N**, and **75.5°E to 80.5°E** as seen in figure 3.2.

The Yamal Peninsula lies within the zone of continuous permafrost, where frozen ground extends to depths exceeding 300 meters. This Arctic lowland, largely composed of wetlands, tundra vegetation, and thermokarst features, is geologically stable yet highly cryosensitive. Key environmental concerns here include:

- Thaw-induced infrastructure damage affecting pipelines and transport corridors
- Methane release from melting permafrost and ground ice
- Subsidence and thermokarst formation, especially in coastal and lowland areas

It is also home to indigenous Nenets communities and traditional reindeer migration corridors. Mapping permafrost in this region has dual relevance: environmental monitoring under climate change scenarios and model benchmarking against a well-studied polar region.

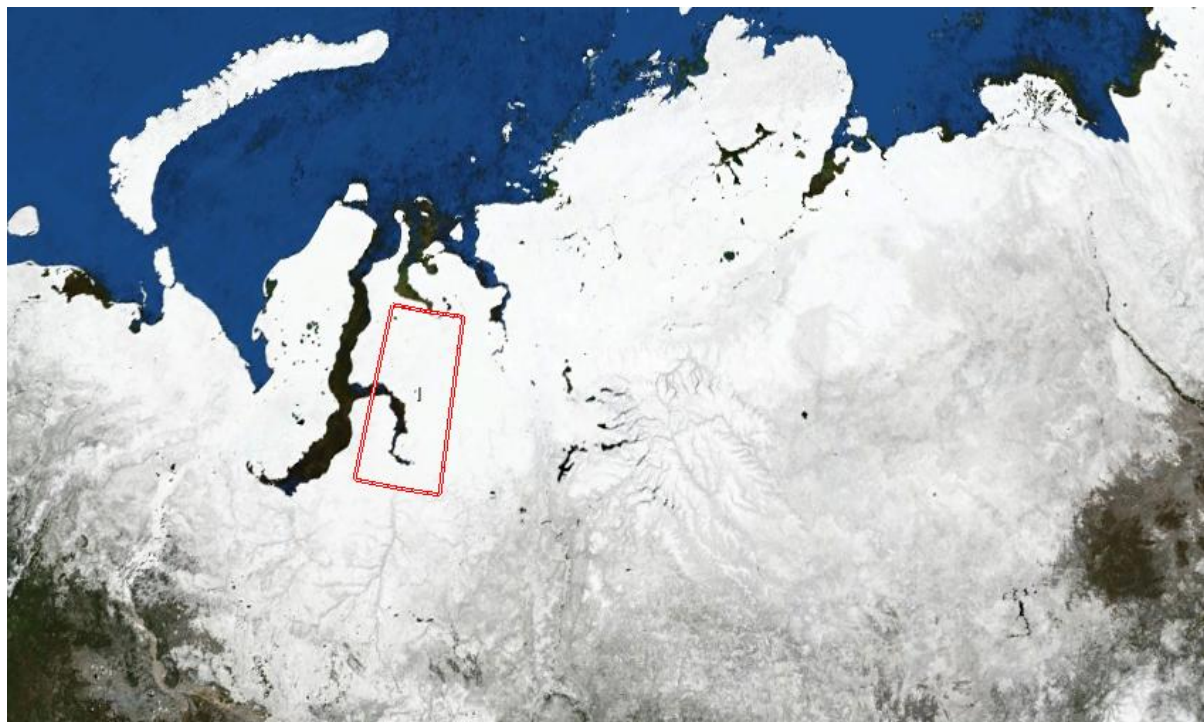


Fig 3.2 ROI Yamal Peninsula

3.2 TERRAIN AND CLIMATE PROFILE

3.2.1 Western Himalayas

1. Topography

The terrain of the Western Himalayas is characterized by:

- Sharp elevation differences ranging from 3,000 to over 6,500 meters
- Tectonically active zones with frequent landslides and slope instability
- Glacial and periglacial features including moraines, rock glaciers, and hanging valleys

The steep and rugged terrain significantly affects microclimates, snow accumulation patterns, and surface energy fluxes, all of which are crucial to permafrost formation and degradation.

2. Climate Characteristics

The Western Himalayas fall under the cold-arid and cold-desert climatic regimes, especially in Ladakh. Key features include:

- Sub-zero temperatures for much of the year (especially above 4,500 m)
- Mean Annual Air Temperature (MAAT) often below -3°C in high-altitude zones
- Low annual precipitation (< 150 mm in some parts) predominantly as snow
- High daily temperature ranges with significant ground freezing at night

Climate variability is also governed by:

- Solar radiation and slope aspect, where south-facing slopes receive more heat
- Seasonal snow cover, which modifies the thermal insulation of the ground
- Wind redistribution of snow, affecting surface heat retention

3. Permafrost Conditions

- Type: Predominantly discontinuous permafrost interspersed with seasonal frost zones
- Ice Content: Varies from negligible to high, depending on valley fill and slope saturation
- Active Layer Thickness (ALT): Ranges between 0.5 to 2.5 meters, depending on terrain and vegetation

Due to the terrain heterogeneity and microclimatic gradients, permafrost can exist even on sunlit slopes if supported by coarse debris or persistent snow. Such complexity demands the use of multi-parametric modeling rather than thermal data alone.

3.2.2 Yamal Peninsula

1. Topography

Unlike the steep terrain of the Himalayas, the Yamal Peninsula is characterized by:

- Broad lowland plains and gentle hills
- Widespread thermokarst depressions and ice wedge polygons
- River valleys and coastal marine terraces shaped by permafrost degradation

The region contains large-scale cryogenic landforms such as pingos, yedoma mounds, and polygonal patterned ground, all of which provide indirect evidence of underlying permafrost processes.

2. Climate Characteristics

- Arctic/Subarctic climate
- Long winters with average temperatures of -20°C to -40°C
- Short, cool summers with daily highs rarely exceeding 10°C
- MAAT ranges from -5°C to -12°C across latitudinal gradients

Snow persists from October to May, and the depth and duration of snow cover affect the soil temperature regime, resulting in highly buffered ground thermal cycles compared to more continental permafrost regions.

3. Permafrost Conditions

- Type: Continuous permafrost with average depths exceeding 250–300 meters
- ALT: Typically between 0.4 to 0.8 meters
- Thaw Impact: Associated with infrastructure destabilization, carbon release, and floodplain expansion

Permafrost in Yamal is more climate-sensitive, but thermally more homogeneous than in the Western Himalayas, making it a suitable test region for validating empirical models

3.3 GROUND VALIDATION AND IN-SITU LIMITATIONS

Challenges in Acquiring In-Situ Data includes ground-based validation of permafrost presence typically involves field installations such as:

- Thermistors or soil temperature probes
- Frost tubes and active layer measurement pits
- Electrical resistivity tomography (ERT)
- Ground Penetrating Radar (GPR)
- Borehole logging and soil coring

However, both the Western Himalayas and Yamal Peninsula pose significant challenges for deploying these methods at scale.

3.3.1 Western Himalayas

The region's remoteness, high altitude, and severe winter conditions limit year-round access. Many areas can only be reached by foot or using helicopter drops, especially during winter. In addition:

- The low oxygen levels at altitudes above 4,500 m restrict prolonged human activity.
- Permafrost zones often lie under rocky debris, making borehole drilling difficult.
- Long-term monitoring requires data loggers and batteries, which degrade quickly in extreme cold.
- Sparse meteorological stations above 3,000 m
- Lack of seasonal soil sampling campaigns
- Security restrictions due to proximity to borders

Consequently, the absence of continuous ground truth data necessitates reliance on proxy models calibrated using global knowledge (e.g., lapse rate, MAAT thresholds, Stefan's Law).

3.3.2 Yamal Peninsula

Although Russia has a history of permafrost monitoring, most boreholes are clustered in urban or oil extraction zones. The following limitations apply:

- Boreholes tend to be logically located near roads and facilities, leaving vast tundra areas unmapped.

- Instrumentation may not align temporally with satellite datasets (e.g., year mismatch between MAGT datasets and MODIS).
- Seasonal flooding and remoteness limit ground surveys during thaw season.

Despite having higher data availability than India, public access to high-resolution, up-to-date permafrost maps with downloadable raster values is limited. Hence, this study primarily relies on open-access satellite data and validated global models, accepting a trade-off between spatial coverage and ground accuracy.

3.4 RASTER AND REANALYSIS DATASETS USED

This section describes the full suite of geospatial datasets used for both regions. All raster layers were processed at 30-meter resolution, standardized via resampling, reprojecting, and masking to ensure alignment during analysis.

3.4.1 DEM and Terrain Derivatives (SRTM, ASTER)

1. Purpose

- Determine terrain elevation, slope, and aspect
- Support lapse-rate corrections in climate indices
- Influence surface energy balance and snow persistence

2. Sources

- SRTMGL1 v003 (NASA/USGS) – 30 m elevation
- ASTER GDEM v3 (JAXA/METI) – used where SRTM has voids or striping

3. Processing

- Imported and clipped using Google Earth Engine
- Derivatives (slope and aspect) computed using:
- Exported in GeoTIFF format and resampled (bilinear) to align with modeling grid

4. Relevance

- Slope: Steeper slopes reduce snow accumulation, increase runoff, and affect thawing
- Aspect: Controls solar radiation exposure—key for surface heating

- Elevation: Required for temperature lapse-rate correction in ERA5

3.4.2 MODIS LST and ERA5 (FDD, TDD)

1. MODIS LST (MOD11A2)

- 8-day composite of day-time land surface temperature at 1 km resolution
- Aggregated over 2020–2023 and converted from Kelvin to Celsius using:
- Serves as a proxy for MAAT, used in TTOP and MAGT estimation

2. ERA5-Land Daily (ECMWF)

- Daily air temperature at 2m above ground
- Processed in GEE to compute:
 - Freezing Degree Days (FDD): Sum of temperatures < 0°C
 - Thawing Degree Days (TDD): Sum of temperatures > 0°C

3. Lapse-Rate Correction

- Applied using elevation from DEM and -6.5°C/km lapse rate
- Output raster: Corrected_FDD_30m.tif and Corrected_TDD_30m.tif

3.4.3 Landsat-8 and Sentinel-2 (NDVI, NDSI)

1. NDVI (Vegetation Proxy)

- Satellite: MOD13Q1 (MODIS) or Landsat-8 OLI
- NDVI calculated as:

$$\text{NDVI} = \frac{(NIR - RED)}{(NIR + RED)}$$

- Threshold-based classification used in TTOP's n-factor estimation:
 - NDVI > 0.2 → nf = 0.7 (vegetated)
 - NDVI ≤ 0.2 → nf = 0.5 (bare)

2. NDSI (Snow Insulation Proxy)

- NDSI calculated as:

$$\text{NDSI} = \frac{(GREEN - SWIR)}{(GREEN + SWIR)}$$

- High NDSI → persistent snow → nt = 0.9 (high insulation)
- Low NDSI → exposed surface → nt = 0.6

Used to model surface modifiers in TTOP and seasonal ground insulation.

3.4.4 SoilGrids Global Soil Parameters

1. Parameters Used

- Bulk Density (kg/m³) → affects thermal mass
- Clay (% by volume) → affects water retention and latent heat storage
- Coarse Fragments (% volume) → influence air voids, conductivity

2. Preprocessing

- Extracted at 0–5 cm and 5–15 cm depth ranges
- Resampled from native 250 m to 30 m
- Normalized and input into thermal conductivity equations:

$$K_f = 1.5 + 0.5 \cdot \frac{\rho_b}{1.6} + 0.01 \cdot \text{clay}$$

$$K_t = 0.5 + 0.3 \cdot \frac{\rho_b}{1.6} + 0.005 \cdot \text{clay}$$

- Used in Stefan's Law to estimate ALT.

3.5 PLATFORM AND TOOLS

3.5.1 Google Earth Engine (GEE)

This cloud-based geospatial processing platform is used to perform the following activities:

- Query and filter remote sensing imagery by time, location, and quality
- Derive indices (NDVI, NDSI), terrain parameters, and lapse-corrected ERA5 products
- Export results at custom spatial resolution (30 m)

Benefits:

- No need for local storage of large datasets
- Parallelized processing for multiyear analysis
- Compatible with MODIS, Landsat, Sentinel, SRTM, and ERA5

3.5.2 Python-Based Local Modeling

Custom scripts built using:

- rasterio for reading/writing GeoTIFFs
- NumPy for matrix-based computations
- scikit-image for resampling
- matplotlib and geopandas for visualization

Used for:

- Resampling all rasters to reference DEM
- Computing models (TTOP, MAGT, ALT)
- Normalizing outputs and generating probability maps
- Visualizing maps with overlays

Scripts included checks for NaN, data clipping, and value normalization for valid computation.

3.5.3 GIS and Visualization Tools

- QGIS: For reclassification, slope-shaded overlays, DEM rendering
- GeoPandas: Overlaying place names, polygons, elevation markers
- Matplotlib / Seaborn: Visualization of probability maps and histograms
- Shapely: Geometry operations for spatial masking

Each tool contributed to either preprocessing, postprocessing, or the generation of report-ready visuals.

CHAPTER 4

ARCHITECTURE AND METHODOLOGY

This chapter outlines the system architecture and details the end-to-end methodology for modeling permafrost in high-altitude regions using empirical models (TTOP, MAGT, ALT) derived from satellite and reanalysis data. From terrain and thermal preprocessing to empirical modeling, normalization, classification, and export—each phase is structured to align with geospatial analysis best practices and military usability standards. The outputs feed directly into terrain-aware planning systems and provide a replicable pipeline for other permafrost-prone regions.

4.1 OVERALL SYSTEM ARCHITECTURE

The system architecture of this project serves as the backbone for the permafrost probability mapping framework, enabling a structured flow of data from raw satellite inputs to final classified maps. The overall architecture is composed of six interdependent layers, each addressing a specific stage in the processing and modeling workflow as seen in figure 4.1.

The first layer, known as the Input Acquisition Layer, comprises the raw geospatial and climatic datasets required for permafrost modeling. These include satellite-based land surface temperature (MODIS), vegetation and snow cover indices (from MODIS and Landsat/Sentinel), reanalysis climate data (ERA5-Land daily 2 m temperature), terrain data (Digital Elevation Models from SRTM/ASTER), and soil attributes (from SoilGrids v2.0). Each input represents a unique environmental driver affecting permafrost behavior, including surface thermal conditions, vegetation insulation, ground heat transfer, and orographic control.

Once collected, the data flows into the Preprocessing and Alignment Layer. In this layer, all raster datasets are resampled to a common resolution of 30 meters using bilinear or cubic interpolation techniques to ensure pixel-wise alignment. Masking operations remove clouds, water bodies, or invalid pixels, and all inputs are spatially clipped to the specific region of interest (ROI). Standardization and normalization steps are also applied where necessary—for example, scaling slope and elevation values to a [0, 1] range before using them in models.

The third layer, the Index Derivation Layer, processes intermediate geophysical variables. It includes the derivation of land surface temperature (LST) from MODIS and estimation of mean annual air temperature (MAAT) as a proxy; vegetation indices such as NDVI (Normalized Difference Vegetation Index), and snow indices like NDSI (Normalized Difference Snow Index); terrain derivatives like slope and aspect from the DEM; and lapse-rate corrected thermal metrics such as Freezing Degree Days (FDD) and Thawing Degree Days (TDD) computed from ERA5 temperature data. These indices form the foundational parameters of subsequent permafrost models.

Following this, the Empirical Modeling Layer consists of three specialized models: the Temperature at the Top of Permafrost (TTOP), the Mean Annual Ground Temperature (MAGT), and the Active Layer Thickness (ALT). Each model uses combinations of the indices from the previous layer to calculate geophysically meaningful indicators of frozen ground. For instance, TTOP uses MAAT, snow/vegetation insulation factors, and thermal conductivity, while ALT is derived using Stefan's law with FDD, bulk density, and soil thermal parameters. The MAGT model uses an empirically fitted regression equation involving NDVI, LST, slope, and elevation.

In the Integration and Probability Mapping Layer, these three model outputs are normalized and integrated into a composite probability score, representing the likelihood of permafrost presence. The normalized values of TTOP, MAGT, and the inverse of ALT (i.e., shallow ALT implies high permafrost confidence) are averaged to yield a continuous probability map. This continuous raster is then categorized into high, moderate, and low-confidence zones using empirically derived thresholds.

Finally, the Output and Visualization Layer is responsible for the generation of output products in usable formats. This includes GeoTIFFs of all primary model layers (TTOP, MAGT, ALT), the composite permafrost probability map, and classified binary/trinary masks. Annotated overlays with place names, slope categories, and elevation ranges are generated using GIS tools. These outputs are prepared for downstream use in autonomous vehicle path planning and strategic terrain analysis.

This six-layer architecture provides a flexible and modular foundation to expand permafrost modeling into other regions (such as Russia, Central Asia, or the Arctic) by simply substituting the regional data while retaining the modeling logic.

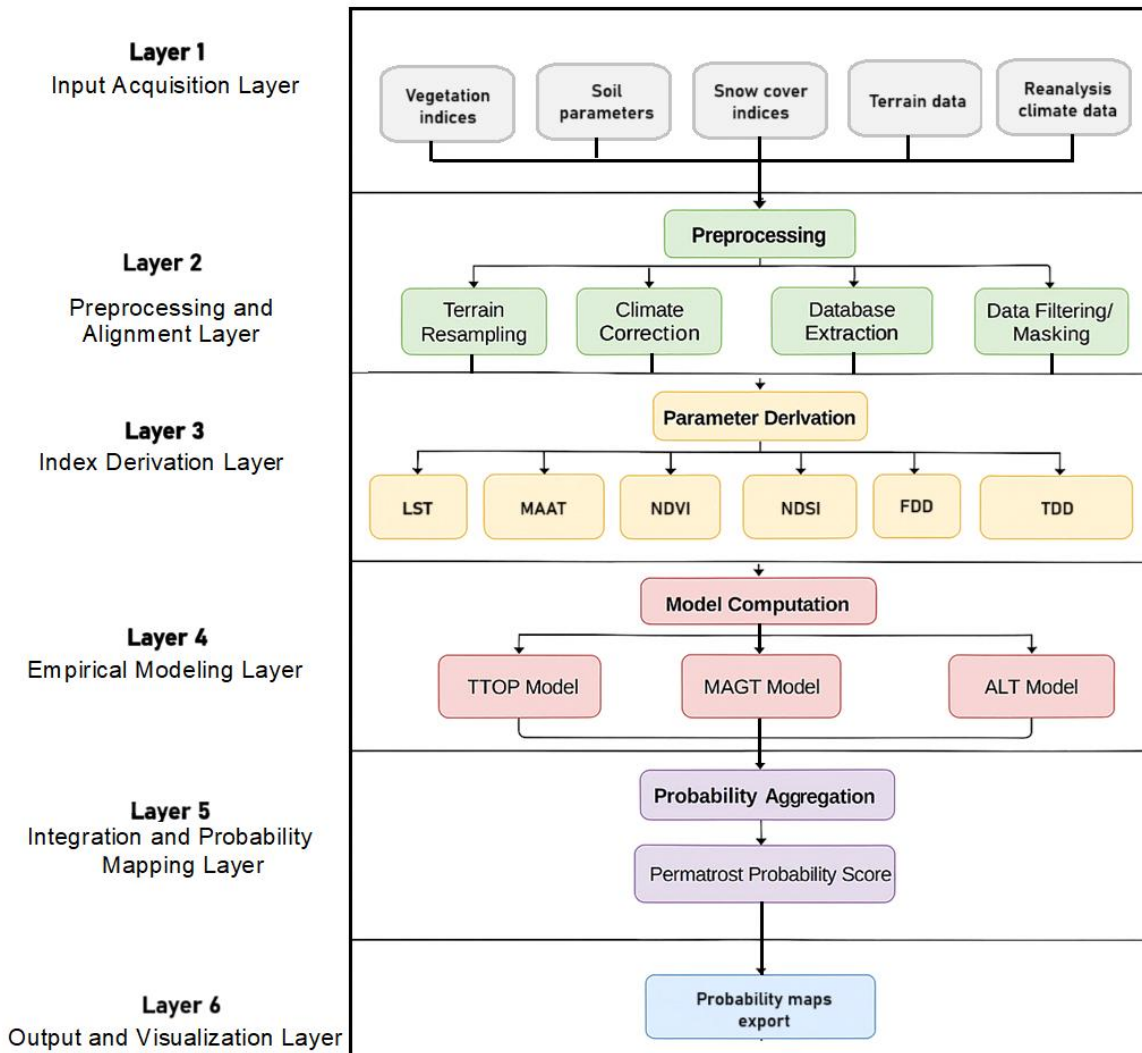


Fig 4.1 System Architecture

4.2 METHODOLOGY

The methodology for permafrost probability mapping follows a well-defined, stepwise framework designed to convert raw environmental raster datasets into empirical thermal models and finally into probability maps. It ensures that each stage starting from raw data acquisition, through preprocessing and modeling, to the final classified outputs can be independently validated and improved as seen in figure 4.2.

The process begins with the collection and preprocessing of all raster inputs required for the modeling. This includes terrain elevation, slope, and aspect data derived from SRTM DEM and ASTER GDEM; thermal measurements from MODIS LST products; climate reanalysis temperature from ERA5; and vegetation/snow cover indices from MODIS MOD13Q1 and Landsat-8/Sentinel-2. All datasets are either downloaded from Google Earth

Engine (GEE) or from public portals like SoilGrids and ECMWF. These datasets inherently come with differing spatial resolutions—MODIS LST (1 km), Landsat NDVI/NDSI (30 m), ERA5-Land (9 km), and SoilGrids (250 m to 1 km). Therefore, before further processing, all datasets are clipped to the Region of Interest (ROI) and resampled to a common 30-meter resolution using bilinear or cubic interpolation. This ensures that all inputs align pixel-to-pixel spatially and can be reliably used in pixel-wise operations during modeling.

Next, the terrain derivatives are extracted. Elevation is directly taken from DEM, while slope and aspect are calculated using `ee.Terrain.slope()` and `ee.Terrain.aspect()` in Google Earth Engine or their equivalent raster operations in Python/QGIS. These terrain attributes influence permafrost distribution in significant ways—steeper slopes generally encourage snow shedding, reducing ground insulation, while aspect determines solar exposure. In the Himalayas, for instance, north-facing slopes retain snow longer and exhibit cooler ground temperatures, increasing the likelihood of permafrost presence.

Following terrain analysis, climate indices are computed, focusing primarily on thermal dynamics. MAAT (Mean Annual Air Temperature) is approximated by converting MODIS LST from Kelvin to Celsius, averaged over the 2020–2023 period. To enhance regional precision, ERA5-Land daily temperature data is used to compute Freezing Degree Days (FDD) and Thawing Degree Days (TDD). Because ERA5 has a coarser resolution (9 km), it is first lapse-rate corrected to match the DEM-derived elevation using a correction factor of $-6.5^{\circ}\text{C}/\text{km}$. FDD is calculated as the sum of daily mean temperatures below 0°C across the full year, while TDD is the sum of daily temperatures above 0°C . These degree-day indices reflect the thermal energy available for ground freezing or thawing, which are directly tied to the thickness of the active layer above permafrost.

The next stage involves the derivation of vegetation and snow cover indicators. NDVI is calculated using near-infrared and red bands, representing the amount and type of vegetation cover. NDVI indirectly serves as a proxy for n-factor (a term used in thermal models that quantifies the surface's thermal resistance based on insulation by vegetation or snow). High NDVI values generally correspond to greater surface insulation and lower ground cooling rates. Similarly, NDSI is derived using green and shortwave-infrared bands and reflects snow presence. Persistent snow can insulate the ground in winter, resulting in warmer soil temperatures despite cold air conditions. Both NDVI and NDSI are used in conjunction to determine surface n-factors for the TTOP model.

Once these variables are derived and spatially aligned, three empirical models are computed independently: TTOP, MAGT, and ALT.

- TTOP (Temperature at the Top of Permafrost) is calculated using the empirical formula:

$$\text{TTOP} = \text{MAAT} \cdot n_f - n_t \cdot \left(\frac{K_t}{K_f} \right)$$

Here, n_f and n_t are freezing and thawing n-factors derived from NDVI and NDSI respectively, while K_f and K_t are the thermal conductivities of the frozen and thawed soil. These conductivity values are estimated using empirical relationships with bulk density and clay content obtained from SoilGrids.

- MAGT (Mean Annual Ground Temperature) is derived using a regression-based model combining surface LST, vegetation index, slope, and elevation:

$$\text{MAGT} = \alpha \cdot \text{LST} + \beta \cdot \text{NDVI} + \delta \cdot \text{Slope}_{\text{norm}} + \epsilon \cdot \text{Elevation}_{\text{norm}} + C$$

Coefficients α , β , δ , ϵ and intercept C are chosen based on calibration to ensure negative correlation with MAGT as elevation and slope increase.

- ALT (Active Layer Thickness) is computed from Stefan's equation:

$$\text{ALT} = \sqrt{\frac{2k \cdot FDD}{L_f \cdot \rho}}$$

where k is the average soil thermal conductivity, FDD is freezing degree days, L_f is the latent heat of fusion of ice (334,000 J/kg), and ρ is soil bulk density. ALT quantifies the depth to which thaw occurs annually and is a critical indicator—low ALT implies high permafrost probability.

Once these three model layers are computed, they are normalized and combined into a unified permafrost probability score. TTOP and MAGT are normalized to [0, 1], and ALT is inverted and normalized (since shallow ALT is favorable for permafrost). The three layers are averaged to produce the final permafrost probability map. Finally, the continuous probability map is classified into three categories:

- High Confidence Permafrost
- Moderate Confidence
- Low/No Permafrost

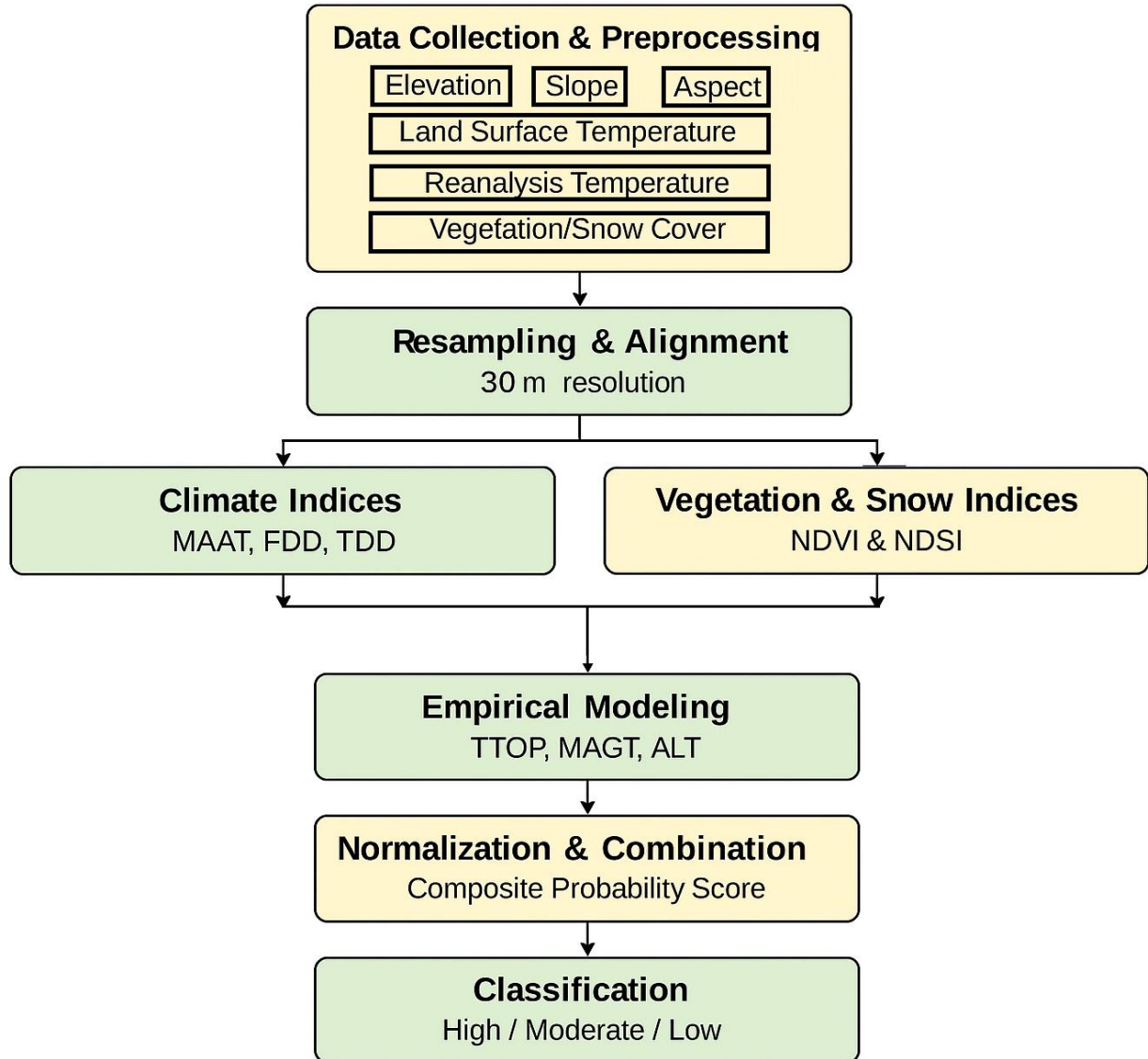


Fig 4.2 Methodology Flowchart

4.3 TERRAIN VARIABLE GENERATION

The first set of physical variables integrated into the permafrost modeling pipeline are terrain-based indices—elevation, slope, and aspect. These factors fundamentally influence ground temperature dynamics and are derived from high-resolution Digital Elevation Models (DEMs) using GIS and remote sensing tools.

- Elevation, derived from SRTM (30 m resolution) and ASTER GDEM (in void regions), provides a direct estimate of terrain altitude. Since atmospheric temperature decreases with height due to the adiabatic lapse rate (approximately $-6.5^{\circ}\text{C}/\text{km}$), elevation plays a critical role in estimating air and ground temperature,

especially when correcting coarse-resolution climate data like ERA5. It also serves as an input to the MAGT regression model and is normalized to integrate into probability mapping.

- Slope is computed from the DEM using raster gradient operations. It represents the steepness of terrain and is measured in degrees. Steeper slopes influence both insulation dynamics and water runoff. Slopes $>45^\circ$ are often excluded from practical path planning due to vehicle instability, and in permafrost studies, steep slopes often exhibit thinner snow cover due to gravitational redistribution, increasing ground exposure and freeze-thaw sensitivity.
- Aspect, or slope orientation, is another critical modifier of solar insolation. South-facing slopes in the Northern Hemisphere receive more direct sunlight and tend to thaw earlier, while north-facing slopes preserve snow and stay thermally insulated. This difference significantly alters the thermal flux into the ground, making aspect crucial in interpreting LST-derived ground temperatures.

Each of these layers—elevation, slope, and aspect—are first computed using Earth Engine or QGIS and resampled to a uniform 30 m grid. They are normalized where necessary and used directly or indirectly in the TTOP, MAGT, and classification components of the model.

4.4 CLIMATE INDEX PROCESSING

Thermal dynamics are central to understanding and predicting permafrost, which fundamentally depends on the heat balance between the atmosphere and the ground. This section outlines how climate-based inputs—specifically Land Surface Temperature (LST), Freezing Degree Days (FDD), and Thawing Degree Days (TDD)—are derived and incorporated.

4.4.1 LST to MAAT Conversion

MODIS MOD11A2 provides 8-day averaged LST data at 1 km resolution. A multi-year mean is computed from 2020 to 2023 using the Google Earth Engine platform. This average is scaled and converted from Kelvin to Celsius. Although LST represents surface skin temperature (not air temperature), it serves as a viable proxy for MAAT, particularly in areas lacking in-situ measurements. The assumption is that long-term averaged LST closely follows air temperature trends in barren or sparsely vegetated high-altitude terrains.

This converted MAAT is then used in the TTOP model as the base air temperature component, modulated by n-factors to estimate the top-of-permafrost thermal boundary.

4.4.2 ERA5-Based FDD and TDD Estimation

ERA5-Land is a reanalysis dataset offering daily 2 m air temperature at ~9 km resolution. To make this compatible with the 30 m terrain raster grid, a lapse-rate correction is applied using the DEM. Specifically, ERA5 temperature grids are adjusted pixel-wise using:

$$T_{\text{corrected}} = T_{\text{ERA5}} + \gamma \cdot (H_{\text{DEM}} - H_{\text{ERA5}})$$

where $\gamma = -6.5$ degree C/km, and heights are in meters. Once corrected, daily temperatures are classified as:

- FDD (Freezing Degree Days): Days where $T < 0$ C, summed as absolute values.
- TDD (Thawing Degree Days): Days where $T > 0$ C, summed directly.

These two metrics quantify thermal energy available for freezing and thawing respectively and are critical components in computing ALT via Stefan's law. Both FDD and TDD are exported at 30 m resolution as GeoTIFFs for later use in the Python-based modeling pipeline.

4.5 VEGETATION AND SNOW COVER INDICES

The permafrost models incorporate surface modifiers through vegetation (NDVI) and snow cover (NDSI) indices, both of which alter surface energy balance and ground thermal flux.

4.5.1 NDVI Thresholding for n-factor

NDVI (Normalized Difference Vegetation Index) is derived from MODIS MOD13Q1 or Landsat/Sentinel datasets, depending on cloud coverage and temporal availability. In cold-arid high-altitude terrains, NDVI rarely exceeds 0.5. The following empirical thresholds are applied:

- $\text{NDVI} > 0.2 \rightarrow n_f = 0.7$
- $\text{NDVI} \leq 0.2 \rightarrow n_f = 0.5$

This thresholding helps assign freezing n-factors that modulate the relationship between MAAT and ground temperature in the TTOP model. Higher NDVI corresponds to more insulation, leading to warmer ground for the same air temperature.

4.5.2 NDSI for Snow Cover Effect

It is derived from Landsat 8 (SR_B3, SR_B6) and processed over 2020–2023 to obtain snow extent medians. The thresholds used are:

- $\text{NDSI} > 0.3 \rightarrow n_t = 0.6$

- $\text{NDSI} \leq 0.3 \rightarrow n_t = 0.9$

Here, a lower thawing n-factor implies better insulation from snow, resulting in shallower seasonal thaw. These n-factors are then directly used in the TTOP model to compute the effective subsurface thermal regime.

4.6 SOIL PARAMETER INTEGRATION

Soil properties significantly influence ground heat transfer processes and thus are essential to accurately modeling permafrost behavior. In this study, soil parameters were sourced from SoilGrids v2.0, which provides globally harmonized gridded soil data up to 2 m depth. These include bulk density, clay content, and coarse fragment percentage, all of which affect thermal conductivity and water retention.

4.6.1 Thermal Conductivity Estimation (K_f , K_t)

Thermal conductivity plays a central role in permafrost modeling by determining how easily heat moves through the soil. Two types of conductivities are considered:

K_f (frozen soil conductivity): This reflects how well the soil transfers heat when it is below 0°C. It is typically higher due to ice content acting as a heat conductor.

K_t (thawed soil conductivity): Represents soil conductivity during thawed conditions, which is generally lower due to increased water retention and decreased thermal contact between particles.

The output values are clipped to physically plausible ranges:

- $K_f \in [0.5, 2.5]$
- $K_t \in [0.2, 1.5]$

These parameters are used in the computation of ALT (Active Layer Thickness) and indirectly influence the TTOP (Temperature at the Top of Permafrost) model through thawing n-factors.

4.6.2 Composite Soil Impact on ALT and TTOP

Soil conductivity, when combined with bulk density, also defines the thermal inertia of the ground. Denser and more conductive soils absorb and release heat faster. This affects:

ALT, through Stefan's Law, where thermal diffusivity is a key variable. TTOP, by adjusting the offset between air and ground temperature using the thawing n-factor derived from NDSI.

Because no in-situ soil moisture data was available, water retention effects were indirectly modeled using the combination of coarse fragments (which reduce retention) and clay content (which increases it). These layers were rasterized, aligned, and used in formulaic models explained in the next section.

4.7 EMPIRICAL MODEL COMPUTATION

This section describes the step-by-step implementation of the three primary permafrost modeling components: TTOP, MAGT, and ALT. Each model uses different parameter combinations and serves a distinct purpose in assessing permafrost thermal regime.

4.7.1 TTOP Equation and Normalization

The Temperature at the Top of Permafrost (TTOP) is computed using the following model:

$$TTOP = MAAT \cdot n_f - n_t \cdot \left(\frac{K_t}{K_f} \right)$$

Where:

- MAAT is derived from MODIS LST (in °C)
- n_f , n_t are n-factors estimated from NDVI and NDSI
- K_f , K_t are thermal conductivities as explained above

This semi-empirical model estimates the temperature at the freezing boundary below the active layer. A negative TTOP ($< 0^\circ\text{C}$) implies stable permafrost conditions. The resulting raster is normalized using:

$$TTOP_{norm} = \frac{TTOP - TTOP_{min}}{TTOP_{max} - TTOP_{min}}$$

This allows the value to contribute equally when integrated with other maps.

4.7.2 ALT Estimation via Stefan's Law

ALT (Active Layer Thickness) represents the depth to which seasonal thawing occurs and is calculated using:

$$ALT = \sqrt{\frac{2 \cdot k \cdot FDD}{\rho \cdot L_f}}$$

Where:

- k = average thermal conductivity = $0.5 \cdot (K_f + K_t)$

- FDD = Freezing Degree Days
- ρ = bulk density
- L_f = latent heat of fusion for water (334,000 J/kg)

Higher FDD implies a deeper freeze, but higher soil density and conductivity can buffer thaw. A threshold of $ALT < 1.5$ m is used to classify high-confidence permafrost zones. ALT is clipped between 0 and 5 meters and also used as an inverse component in the final composite score:

$$ALT_{inv} = 1 - \left(\frac{ALT}{5} \right)$$

4.7.3 MAGT Weighted Empirical Regression

MAGT (Mean Annual Ground Temperature) is approximated using a weighted regression model:

$$MAGT = \alpha \cdot LST + \beta \cdot NDVI + \delta \cdot \text{slope}_{norm} + \epsilon \cdot \text{elevation}_{norm} + C$$

Where empirically tuned coefficients are $\alpha = -1.5$, $\beta = -2.2$, $\delta = -0.5$, $\epsilon = -0.2$, $C = 5.0$.

These values were adapted from literature and validated against known regional thermal behavior. The regression reflects that high NDVI, low elevation, and low slope lead to warmer ground temperatures. The output MAGT is then normalized to [0,1] like the TTOP layer:

$$MAGT_{norm} = \frac{MAGT - MAGT_{min}}{MAGT_{max} - MAGT_{min}}$$

4.8 COMPOSITE PERMAFROST PROBABILITY MAP

Once TTOP, MAGT, and ALT are computed and normalized, the final step is to generate a single probability score for each pixel to represent the likelihood of permafrost presence.

4.8.1 Multi-Criteria Integration

The composite permafrost probability (P) is calculated as:

$$P = \frac{TTOP_{norm} + MAGT_{norm} + ALT_{inv}}{3}$$

This simple average assumes equal weight for each indicator, which is justified given their complementary roles:

- TTOP reflects thermal boundary behavior.
- MAGT captures average sub-surface thermal regime.

- ALT reflects the physical outcome of freeze-thaw energy balance.

4.8.2 Clipping, Scaling, Probability Synthesis

The probability scores are clipped between 0 and 1. They are then classified into:

- High Confidence ($P > 0.7$)
- Moderate Confidence ($0.7 < P \leq 0.4$)
- Low Confidence ($P \leq 0.4$)

Each class is mapped as a different raster layer. These masks are then exported and visualized using color-coded overlays for intuitive interpretation.

4.9 HIGH-CONFIDENCE PERMAFROST MASK

While the composite permafrost probability map provides a continuous likelihood score between 0 and 1, it is often necessary—especially in defense and engineering applications—to classify terrain into binary zones: permafrost likely or permafrost unlikely. To generate a high-confidence binary mask, we rely on a physically interpretable criterion based on the Active Layer Thickness (ALT).

4.9.1 ALT < 1.5 m Rule

Empirical studies across the Arctic, Tibetan Plateau, and Himalayan cryosphere suggest that an ALT less than 1.5 meters generally indicates the presence of underlying perennially frozen ground. This rule is based on:

- Field studies with boreholes showing shallow thaw depths.
- Engineering practice that defines terrain with $ALT < 1.5$ m as hazardous for structural loading and mobility.

In the implemented model, the ALT raster is compared against this threshold pixel-wise: `permafrost_zone = np.where(ALT < 1.5, 1, 0)`. This produces a binary raster where:

- 1 indicates presence of probable permafrost.
- 0 indicates absence or uncertainty.

This high-confidence zone is particularly valuable for path planning systems where such terrain is considered non-traversable or flagged as no-go regions in autonomous navigation logic. The binary mask is exported as a GeoTIFF with a resolution of 30 meters, aligned spatially with the probability raster.

4.10 OVERLAY OF NAMES AND TERRAIN LABELS

Visual validation and communication of spatial outputs benefit from annotated maps

that contextualize the results. In this project, major strategic locations and villages in Ladakh were manually overlaid on the generated maps for clarity.

Implementation Details:

- Place coordinates were extracted for settlements such as Leh, Kargil, Diskit, Pangong, Sumur, etc.
- Geographic points were projected to raster coordinates using the raster transform matrix from rasterio.
- Labels were added using matplotlib.pyplot.text() with adjusted font size and offset to prevent overlap.

This overlay serves multiple purposes:

- Provides human-readable orientation for defense planning.
- Enables region-specific interpretation of permafrost zones.
- Supports decision-making by correlating known infrastructure (e.g., roads, helipads) with terrain stability risks.

The annotated maps were exported as high-resolution PNG images and included in reports and presentations.

CHAPTER 5

IMPLEMENTATION

The implementation phase of this project transforms the theoretical modeling framework into a practical geospatial analysis pipeline that systematically processes satellite, terrain, climate, vegetation, and soil data to generate high-resolution permafrost maps. This chapter details the entire execution workflow from data acquisition to raster generation, model application, and visual interpretation. This section emphasizes the computational realization of the models using cloud-based and local processing environments.

5.1 GEE FOR RASTER GENERATION

5.1.1 Data Collection and Filtering

The first stage in the implementation of the permafrost mapping framework involves the collection and preparation of satellite datasets using Google Earth Engine (GEE). GEE is a cloud-based platform that provides access to a vast library of remote sensing imagery and planetary-scale geospatial datasets. It enables high-speed processing and temporal filtering of imagery from different satellite missions, which are central to permafrost modeling.

For this project, the Region of Interest (ROI) for India was set as a rectangle bounded between longitudes 75.5°E to 80.5°E and latitudes 28.5°N to 36.5°N. The Russian ROI extended between 75.5°E to 80.5°E and 67.0°N to 71.0°N. Within each region, the following datasets were extracted:

- DEM (SRTM 30 m) for elevation, slope, and aspect.
- MODIS MOD11A2 for Land Surface Temperature (LST).
- MODIS MOD13Q1 for NDVI (vegetation cover).
- LANDSAT 8 SR for Normalized Difference Snow Index (NDSI).
- ERA5-Land Daily Aggregated for 2m temperature to derive FDD and TDD.

Each dataset was filtered by:

- Time Period: January 1, 2020 – December 31, 2023.
- Cloud Cover: For Landsat, only images with <10% cloud cover were retained.

- Spatial Resolution: Native resolutions were preserved until final export, after which resampling was done to 30 m.

5.1.2 Terrain Derivation, LST Averaging, NDVI/NDSI Extraction

Once collected, terrain parameters (slope and aspect) were derived using the `ee.Terrain.products()` function from the clipped DEM. For MODIS LST, an 8-day composite average was computed across the full temporal window to obtain a stable and seasonally neutral value.

NDVI was calculated as the maximum seasonal value from MODIS NDVI composites to reflect the peak vegetation period, which helps in inferring ground insulation behavior. Similarly, the NDSI index was derived using median composites from cloud-free Landsat 8 images during winter periods to estimate the influence of persistent snow cover.

All outputs were visualized in GEE to verify quality and were then exported to Google Drive at 30 m resolution in GeoTIFF format using `Export.image.toDrive()` commands.

5.1.3 ERA5-Based FDD/TDD Calculation Using Lapse Rate

One of the most critical steps is the estimation of Freezing Degree Days (FDD) and Thawing Degree Days (TDD), which are essential thermal indices in permafrost studies. These were derived from ERA5-Land daily air temperature data by performing the following steps:

- Convert temperature from Kelvin to Celsius.
- Apply a lapse-rate correction of $-6.5 \text{ }^{\circ}\text{C}/\text{km}$ based on the DEM to account for elevation differences between coarse ERA5 grids (9 km) and local terrain features.
- Generate two raster collections:
 - $\text{fdd} = \text{sum of daily temp when temp} < 0\text{ }^{\circ}\text{C}$.
 - $\text{tdd} = \text{sum of daily temp when temp} > 0\text{ }^{\circ}\text{C}$.

These were reduced over the study period (2020–2023) and exported as high-resolution 30 m rasters after spatial re-projection and resampling.

5.2 PYTHON-BASED MODELING PIPELINE

After obtaining preprocessed raster datasets from Google Earth Engine, the next stage involves applying empirical permafrost models using a local Python-based analysis pipeline. This modular pipeline was developed using scientific libraries such as rasterio, NumPy, scikit-image, matplotlib, and GeoPandas, allowing for batch processing and analysis of spatial layers across both Indian and Russian regions at a common resolution of 30 meters.

5.2.1 Resampling and Raster Stack Construction

The first step in the modeling workflow involves creating a consistent raster stack, where all geospatial datasets (climate, terrain, vegetation, snow, and soil) are aligned in pixel shape, spatial resolution, and coordinate system. This alignment ensures that every pixel represents the same ground location across all input layers.

Steps Performed:

- The DEM raster was selected as the reference grid, defining the shape and geotransform (projection, pixel size).
- Other rasters such as LST, NDVI, NDSI, slope, aspect, FDD, TDD, bulk density, sand, silt, clay, and coarse fragments were:
 - Read using rasterio.
 - Resampled to the reference shape using bilinear interpolation (Resampling.bilinear).
 - Nodata values and anomalies were replaced with zeros or statistically derived thresholds to ensure computational stability.
- Raster values were normalized or clipped to appropriate bounds to prevent model divergence (e.g., TDD and FDD capped at 5000).

The stack is then loaded into NumPy arrays and processed pixel-wise to estimate TTOP, MAGT, and ALT.

5.2.2 Permafrost Probability Visualization

After the primary thermal indices were generated, a final permafrost probability map was created using a multi-criteria integration strategy:

$$P = \frac{\text{TTOP}_{\text{norm}} + \text{MAGT}_{\text{norm}} + (1 - \frac{\text{ALT}}{5.0})}{3}$$

Where it is classified as:

- High: $P \geq 0.7$
- Moderate: $0.4 \leq P < 0.7$
- Low: $P < 0.4$

The final map was exported, and histogram distributions were plotted to understand area coverage across classes.

5.3 VISUALIZATION PIPELINE

The visualization pipeline is a critical component of the implementation stage. It transforms numerical raster output into maps that are both interpretable and insightful, particularly for military, research, or environmental monitoring applications. The maps highlight terrain-aware permafrost zones, overlaid with contextual information such as place names, slope regions, or DEM contours.

5.3.1 Custom Map Plotting with Place Overlays

A series of Python tools including matplotlib, GeoPandas, and shapely were used to:

- Render the permafrost probability map and derived outputs (ALT, TTOP, MAGT).
- Plot latitude/longitude-based place markers for locations such as Leh, Kargil, and Diskit in India; and Salekhard, Nadym, and Gyda in Russia.
 - Each location was:
 - Transformed from geographic to raster coordinates using the inverse of the raster's affine transform.
 - Annotated using `ax.text()` with high-contrast labels.

Map overlays help contextualize model outputs, making the maps actionable for logistics and route planning.

Color Maps and Legends:

- ALT: magma, range [0–5 m]
- MAGT & TTOP: coolwarm, range [-20°C to +20°C]
- Probability map: plasma, range [0 to 1]

A legend and scale bar were included using `matplotlib.colorbar` and `grid` tools to improve map readability.

5.3.2 Layer-Specific Color Palettes

Different layers required suitable palettes for intuitive interpretation:

- TTOP: coolwarm or RdBu diverging palette to capture below-freezing vs above-freezing regions.
- MAGT: Same as TTOP, highlighting subtle shifts in mean annual ground temperature.
- ALT: Sequential palette (magma or YlOrRd) indicating increasing thaw depth.
- Probability Map: plasma or viridis, with classification overlays.
- Classification Mask: Custom colormap using ListedColormap:

- 0 (Low) → gray
- 1 (Moderate) → orange
- 2 (High) → dark red

Each plotted figure was saved as .png and included titles, legends, and annotations. Maps were produced at both full scale and downsampled (zoomed in by 10x or 20x) for printing and inclusion in reports.

5.4 INDICATORS AND THEIR MEANING

5.4.1 Active Layer Thickness (ALT)

- Definition: ALT is the maximum seasonal thaw depth above permafrost; it is the thickness of the ground layer that freezes and thaws annually.
- Interpretation for Permafrost Mapping:
 - Low ALT (<1.5 m): Strongly suggests presence of underlying permafrost—ground stays frozen below this depth.
 - High ALT (>2.5–3 m): Likely absence of permafrost or highly degraded/patchy permafrost.
- Advantages:
 - Directly represents the depth to stable frozen ground.
 - Readily interpretable for infrastructure and terrain stability.
- Limitations:
 - Sensitive to surface conditions, vegetation, snow cover, and soil moisture.
 - Can be misestimated in regions with thick organic layers or taliks (unfrozen ground within permafrost).
 - ALT mapping from remote sensing relies on accurate FDD, soil, and temperature inputs.

5.4.2 Mean Annual Ground Temperature (MAGT)

- Definition: MAGT is the average ground temperature at a specific depth (often at or just below the permafrost table) over a year.
- Interpretation for Permafrost Mapping:
 - MAGT < 0°C: Strong indicator of permafrost (by definition, ground remains below 0°C year-round).
 - MAGT ≈ 0°C: Transition zone; may indicate sporadic, patchy, or warming permafrost.
 - MAGT > 0°C: Absence of permafrost.

- Advantages:
 - Physically robust, integrates annual heat budget and climatic controls.
 - Directly related to permafrost thermal state.
- Limitations:
 - Field measurement at depth is challenging—remote estimation requires assumptions or empirical relationships.
 - Influenced by thermal regime, ground insulation, and hydrology.

5.4.3 Temperature at the Top of Permafrost (TTOP)

- Definition: TTOP is the mean annual temperature at the upper surface of perennially frozen ground (just below the active layer).
- Interpretation for Permafrost Mapping:
 - TTOP < 0°C: Confirms presence of permafrost.
 - TTOP > 0°C: Indicates absence of permafrost.
 - TTOP near 0°C: Marks the transition between permafrost and seasonally frozen ground.
- Advantages:
 - Incorporates both atmospheric forcing (climate) and ground thermal properties (surface/subsurface n-factors).
 - Used as a central parameter in physically-based permafrost models (e.g., TTOP model).
- Limitations:
 - Requires accurate degree-day and n-factor inputs; sensitive to snow, vegetation, and surface cover.
 - Sometimes difficult to parameterize regionally from satellite alone.

5.4.4 Justification for Combining All Three Indicators

- Complementary strengths:
 - ALT reflects annual freeze–thaw dynamics.
 - MAGT captures the mean energy state at depth.
 - TTOP represents the boundary condition at the top of permafrost, integrating surface and subsurface thermal conditions.
- Reduces false positives/negatives:
 - ALT alone can miss warm permafrost or taliks.
 - MAGT/TTOP alone may misclassify thin/patchy permafrost or areas with

- anomalous insulation.
- Combining indicators mitigates the risk that an anomaly or uncertainty in one input will distort the map.
 - Captures transition and marginal zones:
 - Permafrost probability is not binary—transition regions, patchy permafrost, or zones undergoing change are better resolved when all three indices are considered.
 - Robustness: By normalizing and averaging the contributions of all three, the resulting probability index accounts for both surface (ALT) and subsurface (MAGT, TTOP) thermal regimes, leading to higher confidence in detected permafrost zones.
 - Physical consistency: A true permafrost region should have a thin active layer, sub-zero annual ground temperature, and negative TTOP. If any of these fails, the probability of permafrost decreases—reflecting reality.
 - Consensus mapping: Your formula mathematically ensures that a region only scores high if all three indicators agree, which is a common approach in ensemble or consensus-based permafrost probability modeling.

By integrating ALT, MAGT, and TTOP into a composite permafrost probability index, we leverage the unique strengths of each thermal indicator while minimizing their individual weaknesses. This approach provides a more robust and physically grounded estimate of permafrost likelihood, particularly in complex or marginal terrain where permafrost is highly variable. Combining these datasets as in our formula supports nuanced, probabilistic mapping and enhances the reliability of permafrost delineation for both scientific understanding and engineering applications.

CHAPTER 6

RESULTS AND EVALUATION

6.1 RASTER PREPROCESSING AND ALIGNMENT

To enable accurate terrain and permafrost modeling, all raster datasets were resampled and spatially aligned to match the base Digital Elevation Model (DEM), which was set to a 30-meter resolution. This ensured consistency across input layers during composite analysis and modeling. The resampling process used bilinear interpolation for continuous data such as Land Surface Temperature (LST), NDVI, NDSI, slope, aspect, and soil texture layers. A custom Python function was implemented using rasterio for this purpose as discussed in the previous chapters.

For categorical rasters such as binary masks or permafrost zone classifications, nearest-neighbor resampling was used to preserve class integrity. Freezing Degree Days (FDD) and Thawing Degree Days (TDD), available at a coarser resolution, were resized using skimage.transform.resize. Any NaN values introduced during resampling were replaced with zeros using np.nan_to_num to avoid invalid input during computation. Each raster was then clipped and aligned to the DEM grid using the same coordinate reference system and bounding box. This alignment step was verified visually using QGIS and programmatically by comparing metadata and raster dimensions. Figures 6.1 to 6.5 show the aligned environmental and terrain rasters including MODIS LST, NDVI, NDSI, slope, and aspect respectively for India 75.5°E to 80.5°E, 36.5°N to 32.5°N to show as sample. These represent surface conditions that influence ground temperature and insulation. Figures 6.6 to 6.8 show the soil property rasters including bulk density, clay and coarse fragment content respectively for India 75.5°E to 80.5°E, 36.5°N to 32.5°N to show as sample as well. These are key parameters for modeling ground thermal conductivity and active layer thickness. Once aligned, these datasets served as input layers for the permafrost modelling. The formulas associated are as follows:

- **MODIS LST** (Land Surface Temperature): Used to estimate surface temperature conditions relevant for permafrost modelling as observed in figure 6.1.

$$T_{\text{Celsius}} = T_{\text{MODIS}} - 273.15$$

T_{MODIS} = Surface temperature from MODIS (in Kelvin)

T_{Celsius} = Converted temperature (in °C)

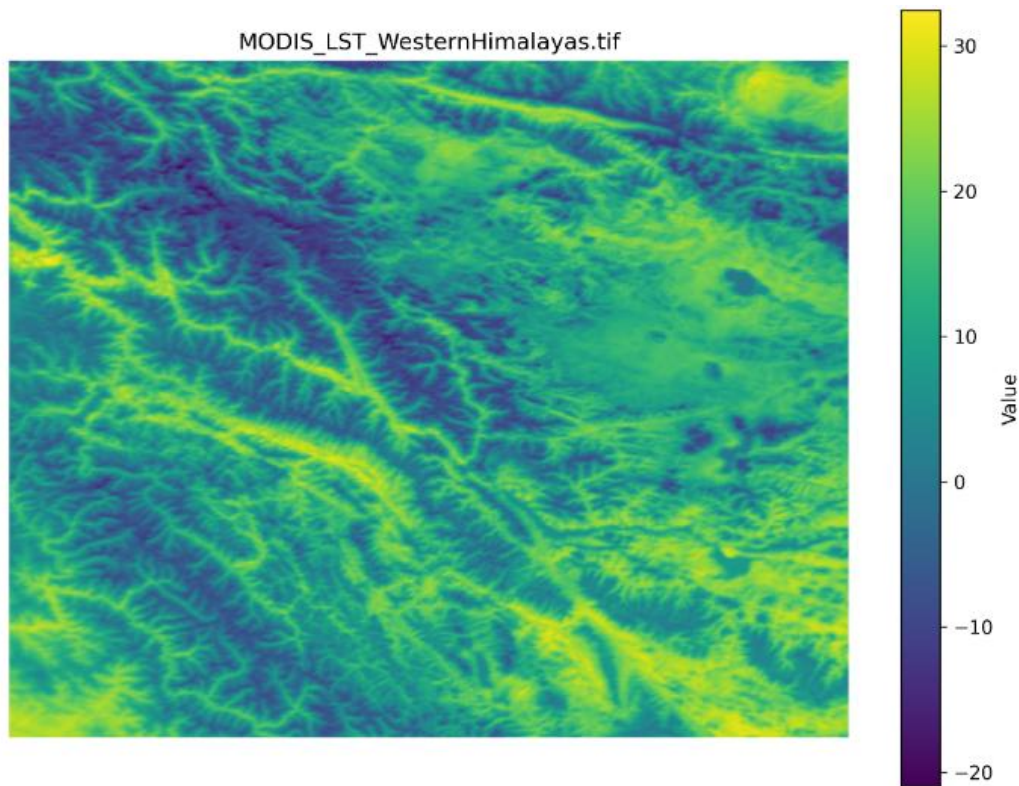


Fig 6.1– MODIS Land Surface Temperature

- **NDVI** (Normalized Difference Vegetation Index): Used to indicate vegetation health and ground insulation potential as observed in figure 6.2.

$$\text{NDVI} = \frac{\text{NIR} - \text{RED}}{\text{NIR} + \text{RED}}$$

NIR = Near-infrared reflectance

RED = Red band reflectance

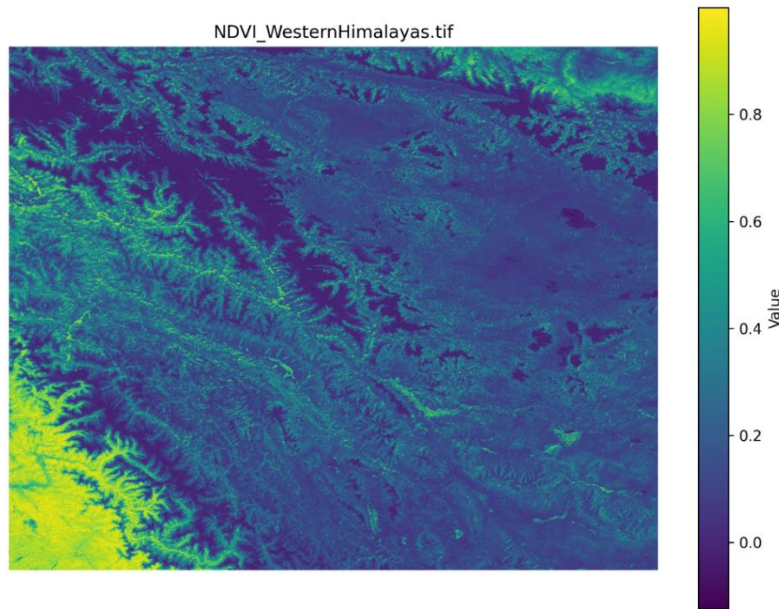


Fig 6.2 – Normalized Difference Vegetation Index

- **NDSI** (Normalized Difference Snow Index): Helps detect snow-covered areas influencing surface energy balance as observed in figure 6.3.

$$\text{NDSI} = \frac{\text{GREEN} - \text{SWIR}}{\text{GREEN} + \text{SWIR}}$$

GREEN = Green band reflectance

SWIR = Shortwave infrared reflectance

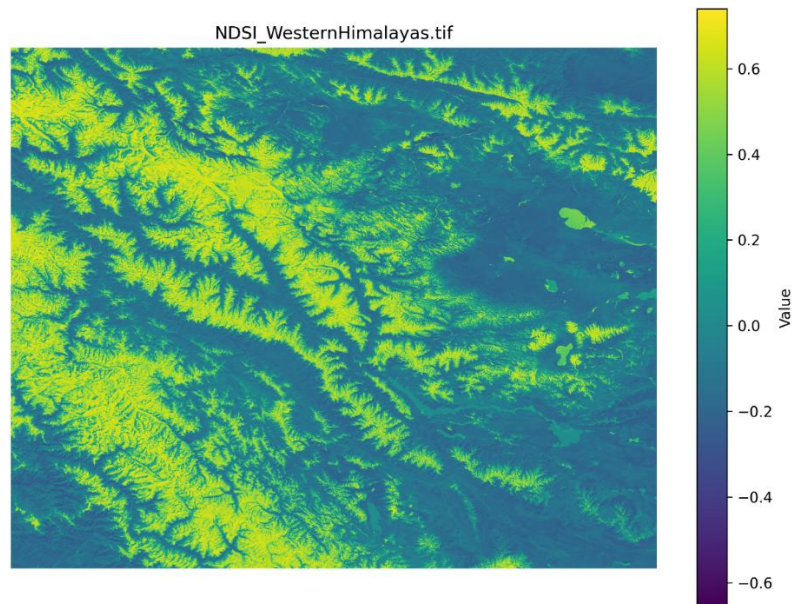


Fig 6.3 – Normalized Difference Snow Index

- **Slope Calculation:** Used to determine terrain steepness from the DEM as observed in figure 6.4.

$$\text{Slope} = \sqrt{\left(\frac{dZ}{dx}\right)^2 + \left(\frac{dZ}{dy}\right)^2}$$

dZ/dx = Elevation gradient in the x-direction

dZ/dy = Elevation gradient in the y-direction

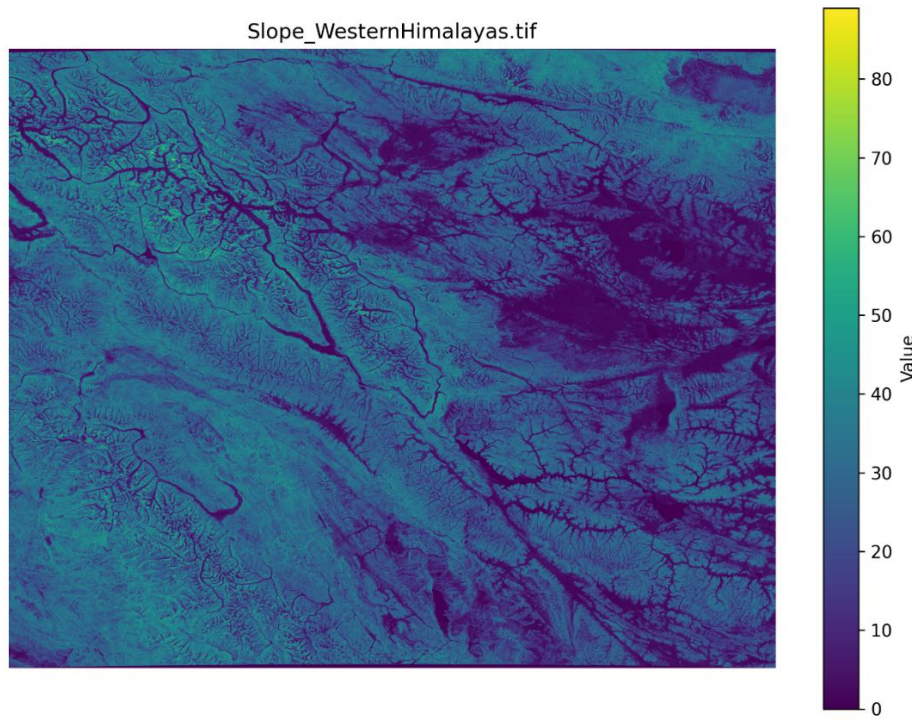


Fig 6.4 – Terrain slope

- **Aspect:** Used to identify slope direction affecting the sun exposure and snowmelt as observed in figure 6.5.

$$\text{Aspect} = \tan^{-1} \left(\frac{\frac{dZ}{dy}}{\frac{dZ}{dx}} \right)$$

Aspect = Direction of steepest slope in degrees (0° – 360°)

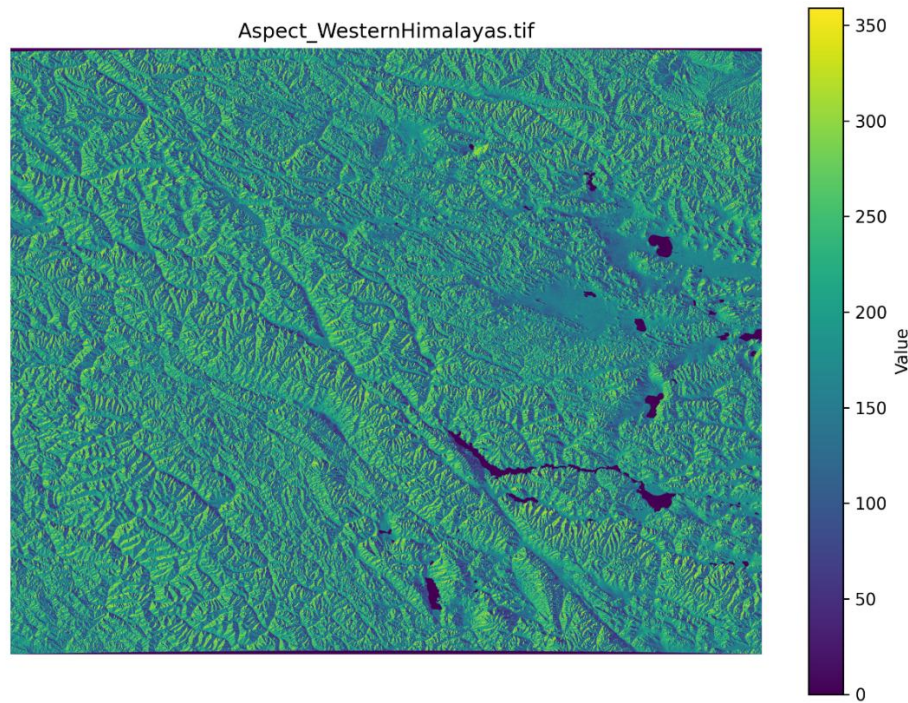


Fig 6.5 – Terrain aspect

- **Frozen Soil Thermal Conductivity:** Calculated to estimate heat transfer through soil.

$$K_f = 1.5 + 0.5 \cdot \left(\frac{\rho}{1.6} \right) + 0.01 \cdot C$$

- **Thawed Soil Thermal Conductivity:** Calculated for estimating conductivity in soil.

$$K_t = 0.5 + 0.3 \cdot \left(\frac{\rho}{1.6} \right) + 0.005 \cdot C$$

K_f = Thermal conductivity when soil is frozen (W/m·K)

K_t = Thermal conductivity when soil is thawed (W/m·K)

ρ = Bulk density of soil (g/cm³)

C = Clay content (%)

Figures 6.6 to 6.8 show the soil property rasters including bulk density, clay and coarse fragment content respectively. These are key parameters for modeling ground thermal conductivity and active layer thickness.

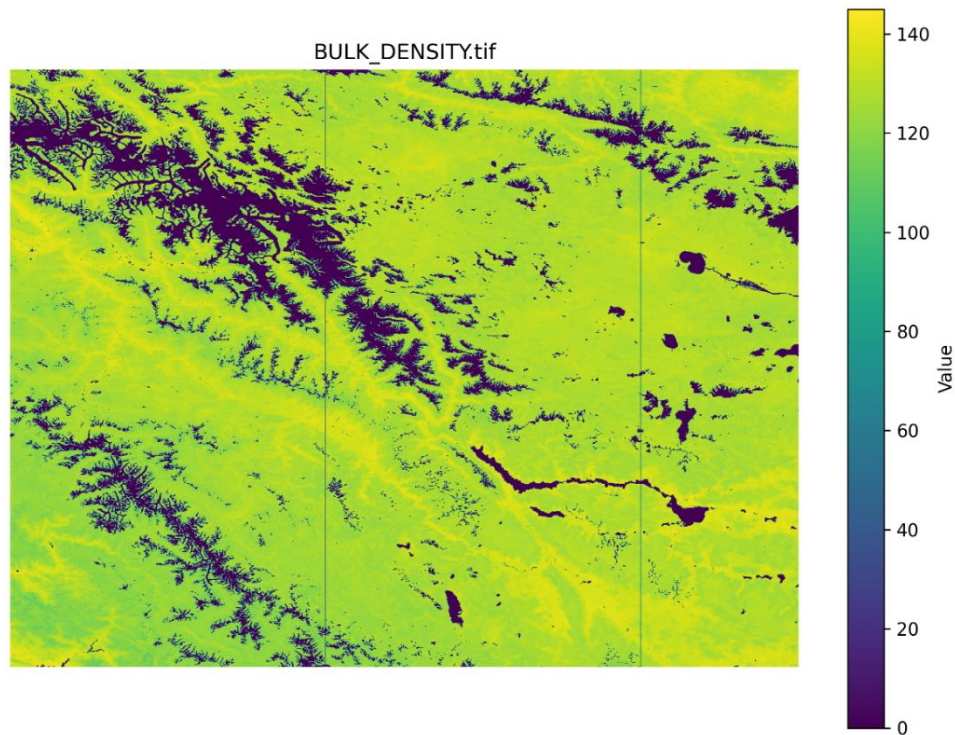


Fig 6.6 – Soil bulk density

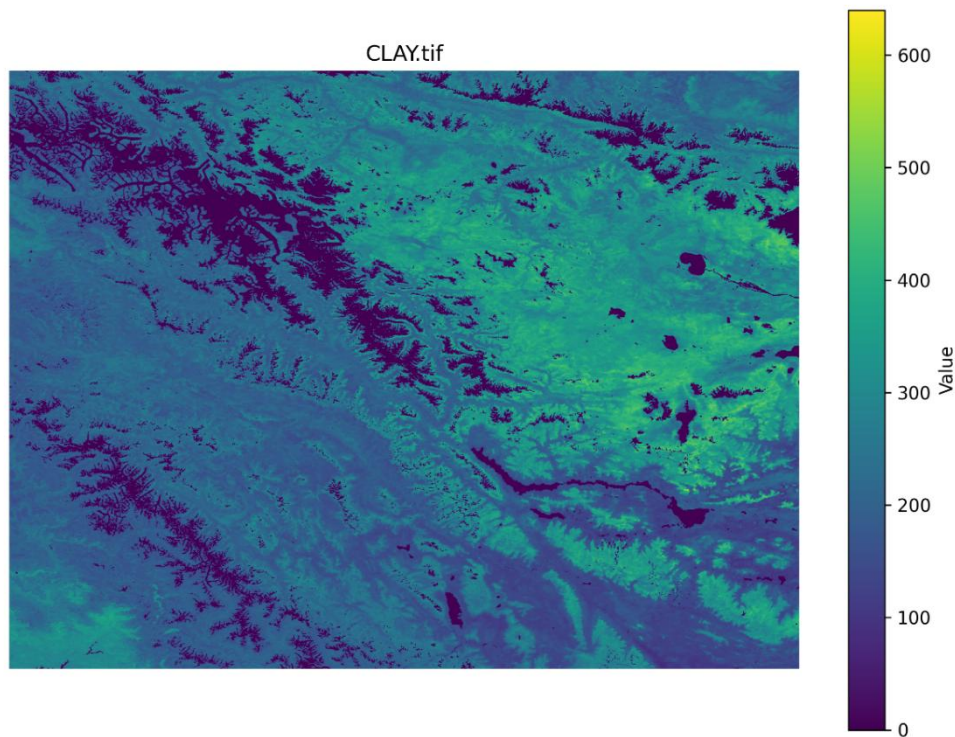


Fig 6.7 – Clay fraction

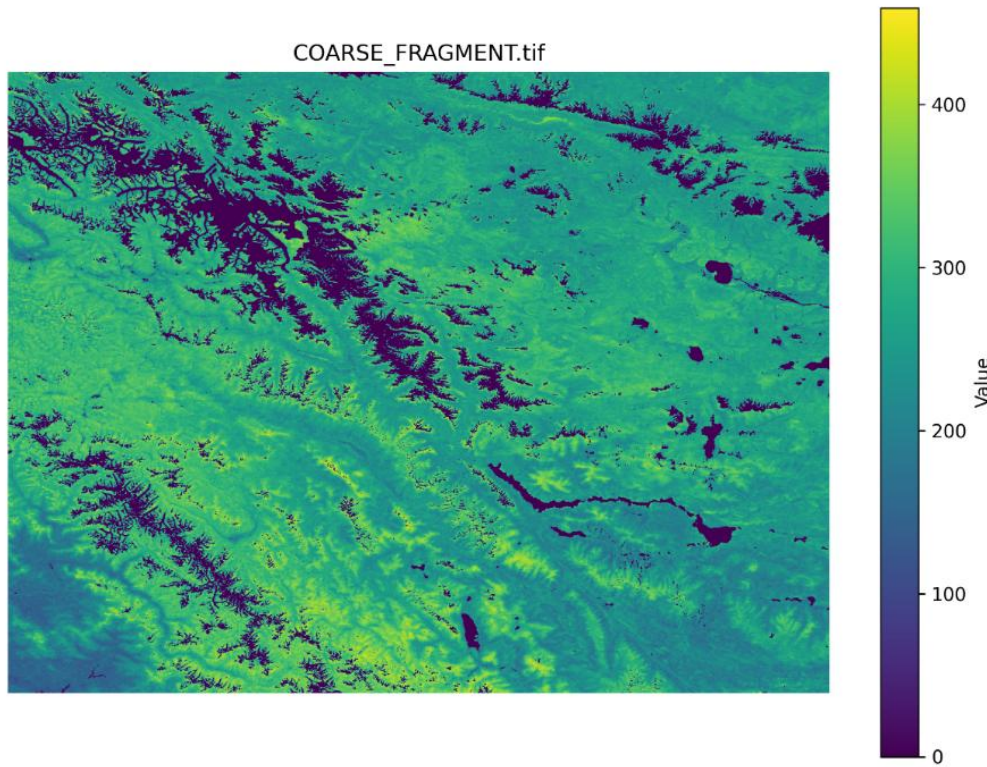


Fig 6.8 – Coarse fragment content

- **Composite Permafrost Probability Map:** Combines multiple permafrost indicators into a normalized probability. All values are scaled between 0 and 1.

$$\text{Probability} = \frac{1}{3} \cdot \left[\left(1 - \frac{\text{ALT}}{5}\right) + \text{Norm}(\text{MAGT}) + \text{Norm}(\text{TTOP}) \right]$$

6.2 PERMAFROST MODELLING

The permafrost modeling process involved the calculation of three key indicators: TTOP (Temperature at the Top of Permafrost), MAGT (Mean Annual Ground Temperature), and ALT (Active Layer Thickness) and their combined composite permafrost probability map along with binary classification map as seen in figures 6.9 to 6.13 for India 75.5°E to 80.5°E, 36.5°N to 32.5°N to show as sample and figure 6.14 shows composite probability map for India 75.5°E to 80.5°E, 32.5°N to 28.5°N while 6.15 shows composite probability map for Russia. These indicators were derived using a combination of satellite datasets and empirical formulas based on thermal and terrain properties relevant to permafrost distribution as discussed in the previous chapters.

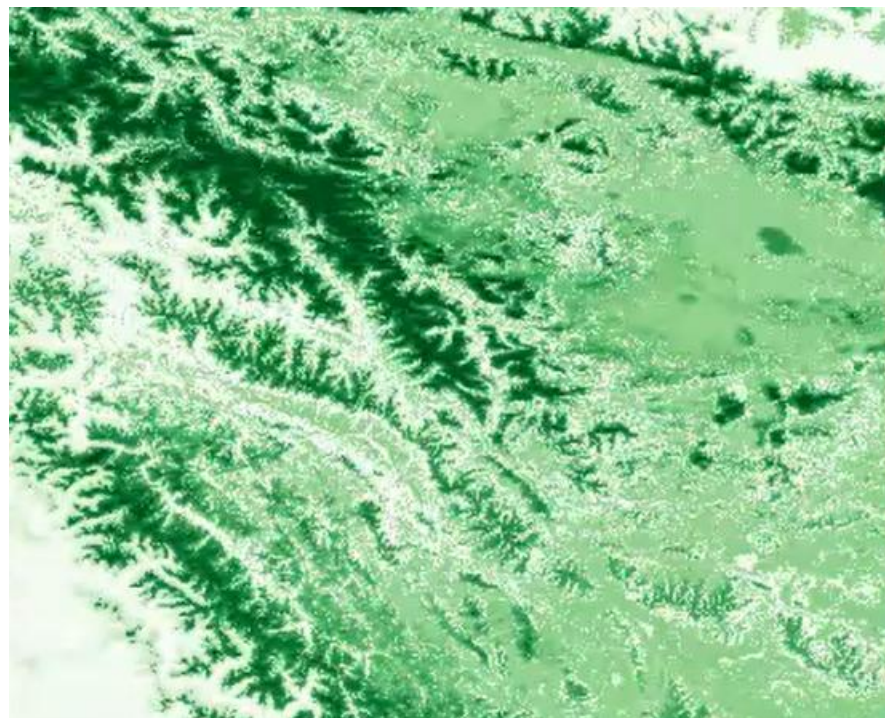


Fig 6.9– ALT map

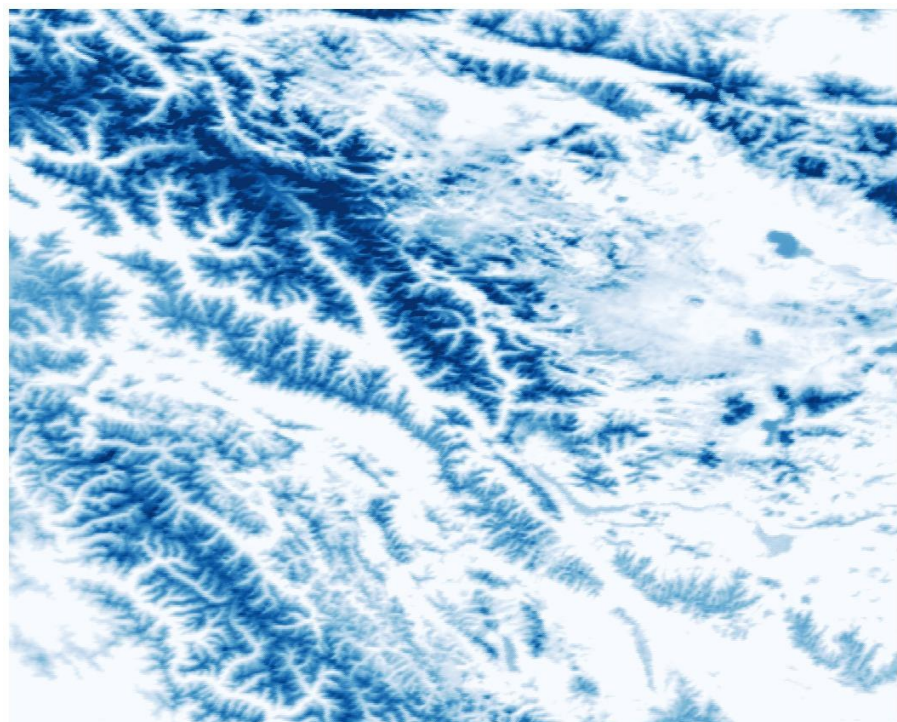


Fig 6.10 – MAGT map (-20 to +20 degree celsius)



Fig 6.11 – TTOP map

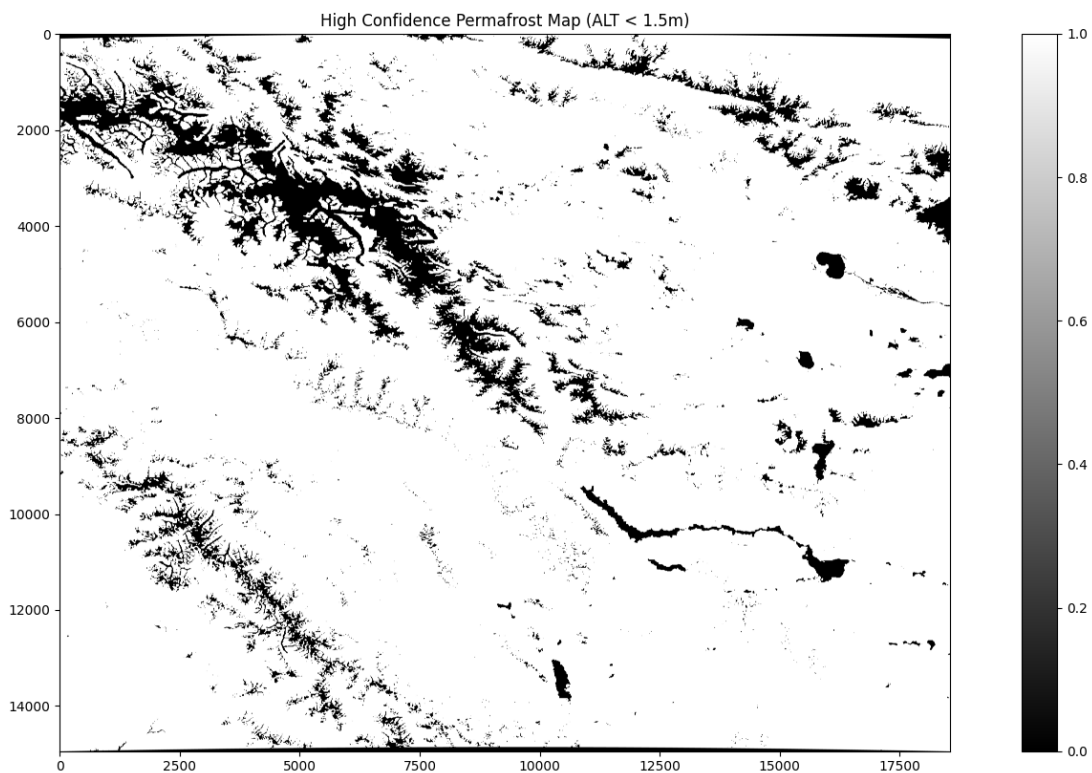


Fig 6.12 – Binary permafrost zone classification

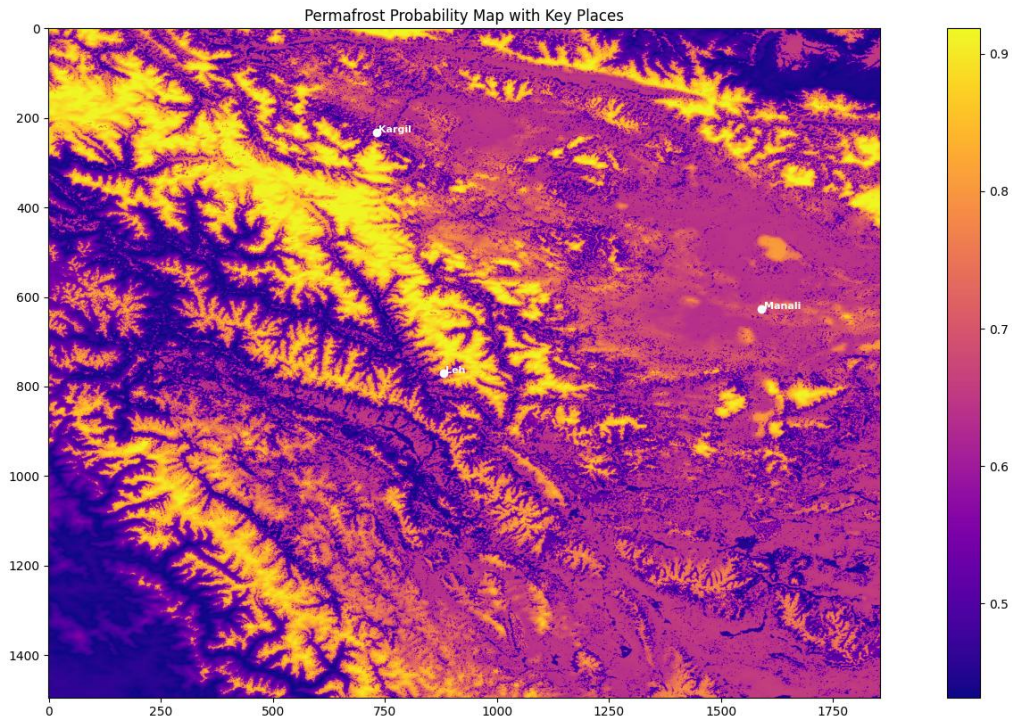


Fig 6.13 – Composite permafrost probability map India 1

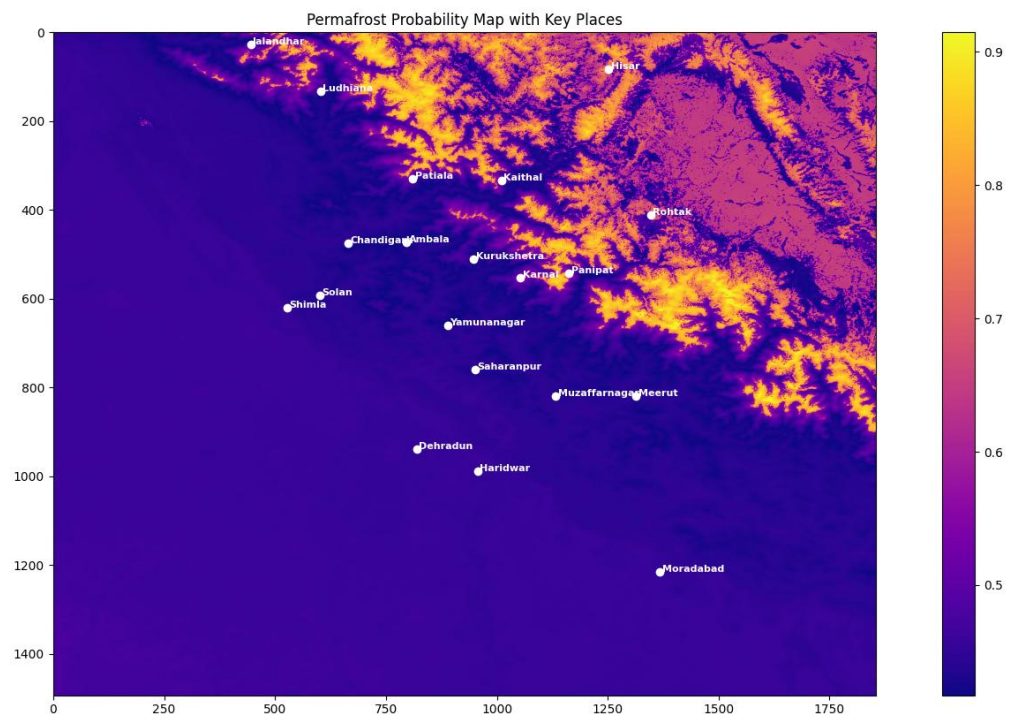


Fig 6.13 – Composite permafrost probability map India 2

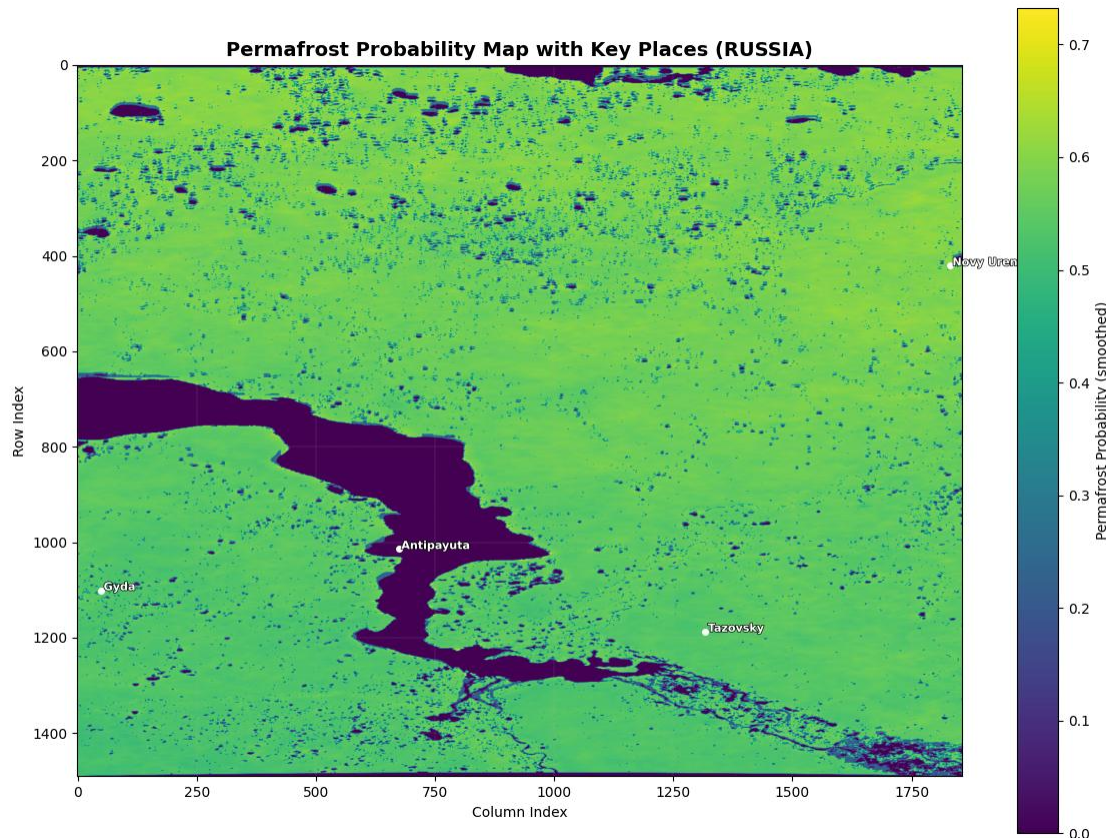


Fig 6.13 – Composite permafrost probability map India 2

6.3 ZONAL CLASSIFICATION

The zonation for each model was based on established literature thresholds and field-calibrated proxies. Classification was carried out using NumPy masking and raster reclassification within the Python modeling environment.

1. TTOP Zones

- TTOP $\leq -2^{\circ}\text{C}$: Very High likelihood of permafrost presence
- $-2^{\circ}\text{C} < \text{TTOP} \leq 0^{\circ}\text{C}$: Moderate likelihood
- TTOP $> 0^{\circ}\text{C}$: Low likelihood or no permafrost

2. MAGT Zones

- MAGT $\leq -1.5^{\circ}\text{C}$: Stable or continuous permafrost zone
- $-1.5^{\circ}\text{C} < \text{MAGT} \leq 0.5^{\circ}\text{C}$: Marginal/discontinuous zone
- MAGT $> 0.5^{\circ}\text{C}$: Likely unfrozen ground

3. ALT Zones

- ALT $< 0.5\text{ m}$: Stable permafrost (perennially frozen)

- $0.5 \text{ m} \leq \text{ALT} < 1.5 \text{ m}$: Seasonal/marginal stability
 - $\text{ALT} \geq 1.5 \text{ m}$: Deep thaw layer; no reliable permafrost
4. Composite Permafrost Probability Zones
- High Confidence (≥ 0.7): Permafrost strongly expected
 - Moderate Confidence (0.4 – 0.7): Potential presence; requires caution
 - Low Confidence (< 0.4): Terrain likely unstable; thaw-dominated

6.4 MAP VERIFICATION WITH GROUND TRUTH

To ensure the reliability of the modeled permafrost indicators—ALT (Active Layer Thickness), MAGT (Mean Annual Ground Temperature), and the derived permafrost probability maps—we conducted a comparative analysis with authoritative global datasets such as those from ESA and NIEER. The focus was to validate spatial correspondence and pattern accuracy across both Indian and Russian regions.

6.4.1 Russia: MAGT Comparison



Fig. 6.14: ESA MAGT Map for Yamal Region, Russia

Fig. 6.14 illustrates the MAGT distribution obtained from the ESA Permafrost CCI dataset for the Russian Yamal region. This dataset represents climatologically averaged MAGT values interpolated using borehole observations and satellite-derived predictors.



Fig. 6.15: Locally Computed MAGT Map using MODIS and Terrain Derivatives

Fig. 6.15 shows the MAGT map generated from our model using calibrated regression on MODIS LST, NDVI, normalized slope, and DEM elevation.

Inference: The spatial temperature gradients show good correlation, particularly in zones with persistent permafrost. Northern regions show low MAGT values (below -5 °C), while southern areas reflect warmer ground conditions. Our model provides finer spatial resolution and better terrain discrimination due to the incorporation of slope and NDVI.

6.4.2 Russia: ALT Comparison



Fig. 6.16: ALT Map from NIEER Database – Russian Permafrost Domain

Fig. 6.16 displays the NIEER-based ALT map representing modeled thaw depths derived from long-term borehole records and numerical simulation.

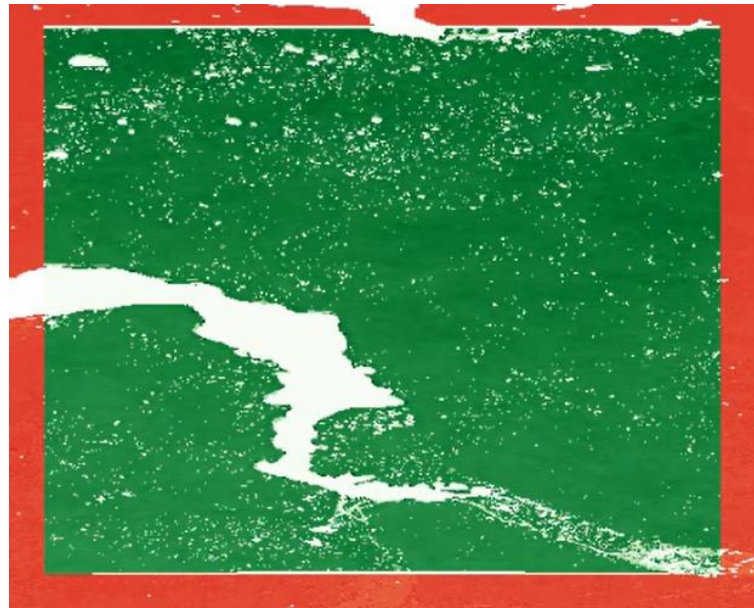


Fig. 6.17: Computed ALT Map from FDD and Soil Thermal Parameters

Fig. 6.17 presents our computed ALT map using the Stefan equation, with FDD, bulk density-based thermal conductivity, and soil parameters.

Inference: The pattern of shallow active layers ($ALT < 1.5$ m) in permafrost-prone zones aligns well in both maps. Notable agreement is observed in the northern tundra zones and riverbank regions. Variations near the southern margin arise due to interpolation differences in NIEER versus our grid-based approach using satellite datasets.

6.4.3 India: ALT Comparison

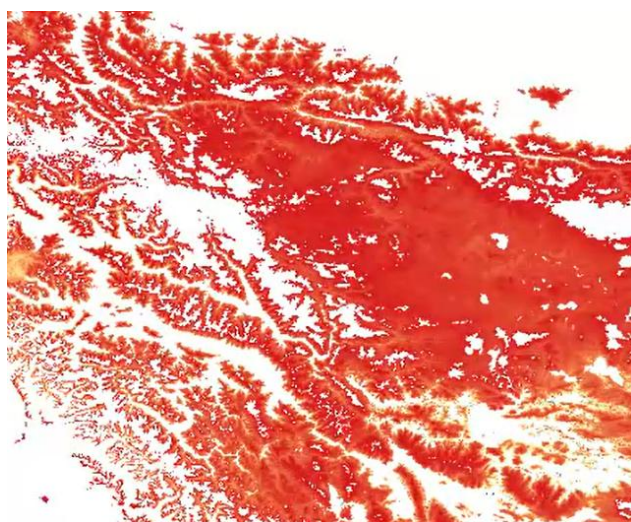


Fig. 6.18: ESA ALT Map for the Indian Western Himalayas

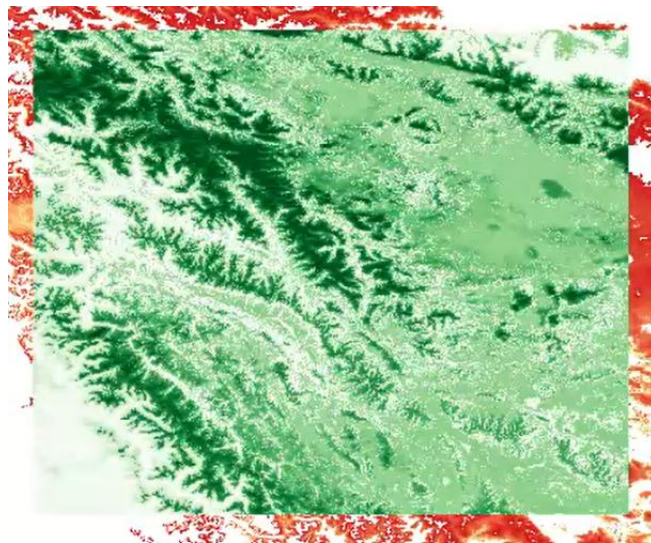


Fig. 6.19: Locally Modeled ALT Map using High-Resolution Climatic and Terrain Inputs

Inference: Our model replicates the ESA trends in ALT depth, especially around Leh, Kargil, and Lahaul-Spiti. Low-ALT zones in our map coincide with high-altitude plateaus and north-facing slopes, reflecting areas of strong permafrost likelihood. Our use of high-resolution inputs enables better detection of local thermal variations within narrow valleys and ridge lines.

6.4.4 India: Composite Probability Comparison

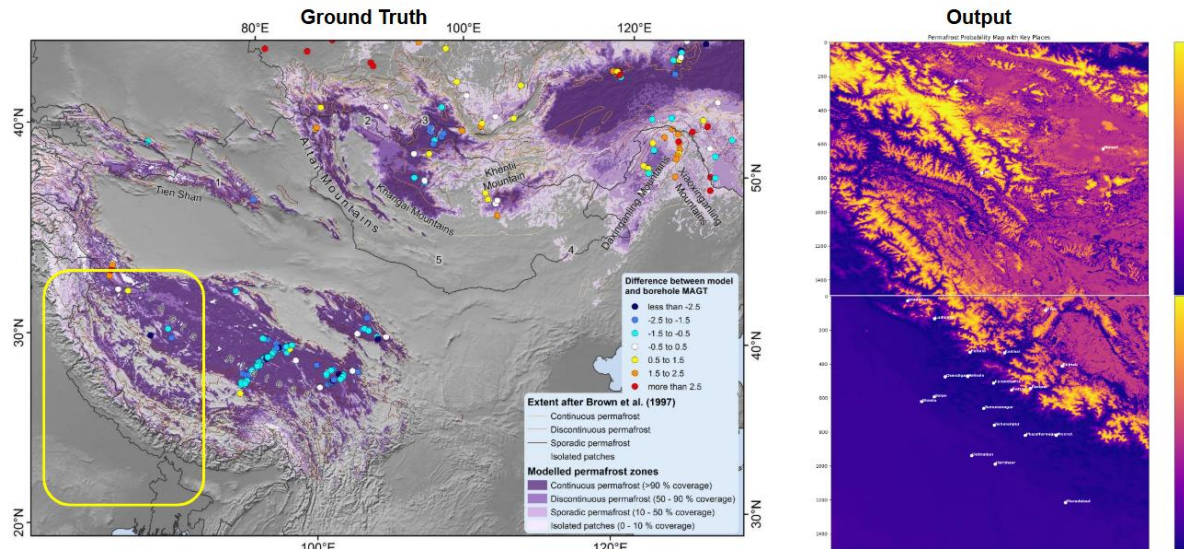


Fig. 6.20: Composite Permafrost Probability Map – Western Himalayas

Fig. 6.20 presents the combined permafrost probability map for the Indian region, based on a weighted integration of MAGT, TTOP, and ALT indicators.

Inference: Regions with high permafrost probability (scores > 0.7) strongly correspond to known cryosphere zones, including Ladakh and upper Lahaul. Compared to standalone ALT or MAGT maps, the ensemble model reduces ambiguity in marginal areas by capturing complementary aspects of thermal state and seasonal thaw dynamics.

6.4.5 Russia: Composite Probability Comparison

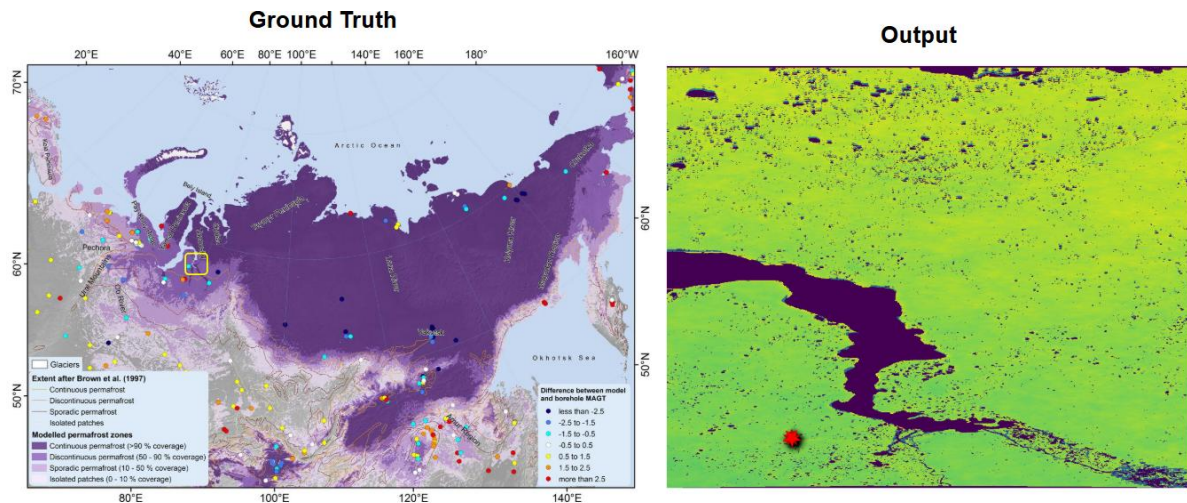


Fig. 6.21: Composite Permafrost Probability Map – Russian Yamal Region

Fig. 6.21 shows the permafrost probability map for the Yamal Peninsula in Russia using our integrated approach.

Inference: Northern Arctic zones (e.g., Sabetta, Tazovsky) show high permafrost stability (scores > 0.85), while transitional bands toward Novy Urengoy and Nadym reflect reduced stability with probability between 0.4 and 0.6. These results match expected gradients and enhance prediction clarity compared to conventional single-variable thresholds.

CHAPTER 7

CONCLUSION AND FUTURE WORK

The objective of this work was to design and evaluate an autonomous terrain-aware path planning system using variants of the A* algorithm, tailored for military logistic applications—specifically, autonomous navigation of tracked tanker vehicles in regions with limited or no road infrastructure. The deployment focus was on high-relief zones such as the Eastern Himalayas, where conventional GPS-enabled navigation is insufficient due to abrupt terrain gradients, slope-induced hazards, and the absence of paved routes.

The proposed system utilized geospatial raster datasets—namely Digital Elevation Models (DEM) and slope maps derived from SRTM and processed via Google Earth Engine (GEE)—to generate terrain-aware cost surfaces. These were used to construct a **probabilistic terrain feasibility map (PTFM)** that informed the navigation logic of enhanced A* variants.

7.1 SUMMARY OF WORK DONE

This study focused on modeling and mapping permafrost probability zones in high-altitude terrains using publicly available satellite and reanalysis datasets, implemented over select regions of the Western Himalayas and Russia. The project aimed to support defense operations and autonomous mobility systems by identifying geotechnically unstable areas through thermal, terrain, vegetation, and soil indices.

Key accomplishments of the study include:

- The creation of 30-meter resolution permafrost probability maps using TTOP, MAGT, and ALT models.
- Integration of satellite-based variables such as MODIS LST, ERA5-derived FDD/TDD, NDVI, NDSI, and terrain derivatives (elevation, slope, aspect).
- Empirical modeling of TTOP using surface modifiers and soil conductivity, MAGT using terrain-climate regressions, and ALT using Stefan's equation.
- Implementation of preprocessing workflows in Google Earth Engine and a modeling pipeline in Python.

- Export of GeoTIFF-based raster outputs, including classified permafrost zones and binary masks indicating high-confidence frozen terrain.
- Integration-ready outputs to be used in path planning algorithms for defense tanker vehicles and autonomous robots operating in permafrost-prone terrains.

The entire system architecture was divided into multiple layers, from data acquisition to final raster synthesis and visualization, ensuring transparency, modularity, and reproducibility.

7.2 KEY OBSERVATIONS

- Spatial Variation: Permafrost presence was highest in north-facing slopes and high-elevation ridgelines above 4,500 m, where the combination of low LST, high FDD, and shallow ALT pointed to ground stability over longer freeze periods.
- Role of Slope and Aspect: Steeper slopes with northern aspects retained higher permafrost scores, especially in zones with lower solar insolation and reduced thawing during summer.
- Vegetation and Snow Influence: NDVI and NDSI thresholds successfully captured insulating and reflective properties, respectively. Vegetated zones with $NDVI > 0.2$ retained frost longer, while snow-dominated zones were more seasonally dynamic.
- Soil Conductivity Impact: High clay and bulk density values indicated stronger thermal buffering and greater variability in thaw depth, influencing both TTOP and ALT.
- ERA5 Bias Correction: Lapse-rate correction of ERA5 data improved thermal estimation fidelity, reducing the elevation mismatch common in global reanalysis datasets.

The multi-model synthesis showed that regions identified as high-confidence zones by all three models ($TTOP < 0^\circ\text{C}$, $MAGT < -2^\circ\text{C}$, $ALT < 1.5 \text{ m}$) were aligned with geomorphologically probable permafrost areas, lending confidence to the methodology.

7.3 LIMITATIONS OF CURRENT STUDY

- Absence of Ground Truth: There is a lack of field validation using borehole data, thermistor probes, or active layer monitoring. While global models provide reference maps, their spatial mismatch and thematic inconsistencies limit full accuracy assessment.
- Static Snapshot: The study represents a temporally averaged state (2020–2023) and does not reflect seasonal or annual variability beyond those bounds. Long-term thaw trends or short-term freeze anomalies are not captured.

- Model Generalization: Empirical models like TTOP and MAGT use assumptions derived from Arctic or sub-Arctic contexts. Their parameters may require fine-tuning for Himalayan or Central Asian conditions.
- Sensor Resolution Constraints: MODIS LST and ERA5 data had to be resampled to 30 m, potentially introducing interpolation errors. Some data layers, like soil grids, had native resolutions around 250–1000 m.
- Snow Dynamics Modeling: Snow cover presence (NDSI) was used as a proxy, but actual snow depth, duration, and thermal conductivity were not directly modeled due to unavailability of high-resolution snow datasets.

7.4 FUTURE SCOPE

To address these limitations and expand applicability, future work can be divided into several technical and operational extensions:

7.4.1 Ground Validation with Borehole and Temperature Loggers

Deploying low-cost data loggers or accessing borehole archives (e.g., CALM, GTN-P, NSIDC) can help validate and calibrate modeled outputs. Comparing measured TTOP, MAGT, or ALT with the modeled rasters across elevation gradients will refine the empirical assumptions and rating weights.

7.4.2 Integration of Machine Learning and SAR Techniques

Machine learning (ML) models can capture nonlinear interactions between variables. Approaches like Random Forest or Gradient Boosting can be trained using borehole data and raster inputs to predict permafrost classes. Synthetic Aperture Radar (SAR) and InSAR-based ground displacement (e.g., Sentinel-1) can be included as indicators of active layer dynamics or subsidence caused by thawing.

7.4.3 Temporal Modeling and Change Detection

Mapping the seasonal freeze–thaw cycle through time-series MODIS or Sentinel data can help build a multi-temporal permafrost model. This would allow tracking of thaw progression, slope destabilization zones, or infrastructure vulnerability trends.

7.4.4 Advanced Snow Parameter Integration

Future versions can incorporate data from snow-specific satellites like AMSR-E, IMERG, or even SnowModel simulations to include parameters like snow depth, density, and thermal diffusivity. These will enhance accuracy of TTOP and MAGT during seasonal transitions.

7.4.5 Coupling with Robotic Path Planning Engines

The classified permafrost probability masks can be directly integrated into ROS 2-based navigation stacks. By using high permafrost zones as no-go regions in costmaps, planners like NavFn, Hybrid A*, or D* Lite can avoid unstable regions during route generation. Simulation trials in Gazebo or RViz can demonstrate operational benefit.

7.4.6 Regional Generalization to Arctic and Polar Terrains

The pipeline, though designed for the Himalayas, can be adapted to permafrost-prone regions like the Yamal Peninsula, Alaska, or Greenland by adjusting parameter weights and model coefficients. Cross-comparisons with Arctic datasets like the Circum-Arctic Map (NSIDC) will aid global scalability.

7.5 CLIMATE MONITORING AND DEFENSE SYNERGY

This study contributes to the dual agendas of climate change adaptation and defense infrastructure management. Permafrost is a climate-sensitive ground feature; changes in its spatial extent, thaw depth, and surface mobility directly signal warming trends in cryospheric zones.

For military logistics and autonomous ground systems, the availability of terrain intelligence derived from such maps helps minimize route failure, fuel wastage, and human exposure in hazardous zones. By converting remotely sensed environmental data into actionable inputs, this work enhances both climate risk modeling and tactical mission support.

7.6 FINAL REMARKS

This report presents a replicable, open-data-driven framework for identifying terrain instability in permafrost zones using globally available satellite inputs. It bridges the gap between geoscientific modeling and autonomous mobility systems in extreme terrains.

While empirical, the pipeline lays a strong foundation for more advanced models combining SAR, AI, and long-term climate projections. As geopolitical and environmental pressures intensify in cryo-sensitive zones, this form of terrain modeling will be essential for ensuring safe, informed, and sustainable deployment of resources—both human and robotic.

BIBLIOGRAPHY

1. M. A. R. Khan, B. S. Sinha, and A. K. Patel, "Modelling Permafrost Distribution in Western Himalaya Using Remote Sensing and Field Observations," *Remote Sensing*, vol. 13, no. 14, pp. 1–22, 2021.
2. D. Luo, Z. Wu, X. Li, and H. Liu, "PIC v1.3: Comprehensive R Package for Computing Permafrost Indices over the Qinghai–Tibet Plateau," *Geoscientific Model Development*, vol. 14, no. 3, pp. 1379–1396, 2021.
3. J. Brown, O. J. Ferrians Jr., J. A. Heginbottom, and E. S. Melnikov, "Circum-Arctic Map of Permafrost and Ground-Ice Conditions," National Snow and Ice Data Center, Boulder, CO, 1997.
4. M. W. Smith and D. W. Riseborough, "Climate and the Limits of Permafrost: A Zonal Analysis," *Permafrost and Periglacial Processes*, vol. 13, no. 1, pp. 1–15, 2002.
5. T. Zhang, R. G. Barry, K. Stamnes, V. Romanovsky, and M. T. Prowse, "Spatial and Temporal Variability in Active Layer Thickness," *Journal of Geophysical Research: Atmospheres*, vol. 110, no. D13, pp. 1–13, 2005.
6. N. Gorelick et al., "Google Earth Engine: Planetary-Scale Geospatial Analysis for Everyone," *Remote Sensing of Environment*, vol. 202, pp. 18–27, 2017.
7. S. Westermann, R. Kumar, and T. J. Frolking, "Remote Sensing of Permafrost and Frozen Ground," *Earth Science Reviews*, vol. 147, pp. 330–354, 2015.
8. T. E. Osterkamp, "Characteristics of the Recent Warming of Permafrost in Alaska," *Journal of Geophysical Research: Earth Surface*, vol. 112, F02S02, 2007.
9. ISRO - National Remote Sensing Centre, "Bhuvan Geoportal," [Online]. Available: <https://bhuvan.nrsc.gov.in>

BIBLIOGRAPHY

10. Wadia Institute of Himalayan Geology (WIHG), "Studies on Permafrost in the Western Himalayas," Technical Report, 2020.
11. A. Negi, S. K. Srivastava, and R. D. Singh, "Snow and Permafrost Studies in Ladakh Using Remote Sensing," *International Journal of Remote Sensing Applications*, vol. 11, no. 2, pp. 45–57, 2021.
12. H. Hersbach et al., "The ERA5 Global Reanalysis Dataset," *Quarterly Journal of the Royal Meteorological Society*, vol. 146, no. 730, pp. 1999–2049, 2020.
13. A. Lewkowicz and J. Bonnaventure, "Permafrost and Climate Change in Canada: An Overview of Recent Research and Future Trends," *Canadian Journal of Earth Sciences*, vol. 45, no. 10, pp. 1213–1230, 2008.
14. G. Hugelius et al., "The Northern Circumpolar Soil Carbon Database: Spatially Distributed Datasets of Soil Coverage and Soil Organic Carbon Storage in the Northern Permafrost Regions," *Earth System Science Data*, vol. 5, no. 1, pp. 3–13, 2013.
15. M. Jafarov, V. E. Romanovsky, and J. E. Walsh, "Permafrost Degradation and Modeled Soil Carbon Loss in the West Siberian Arctic Region," *Geophysical Research Letters*, vol. 39, no. L05503, pp. 1–6, 2012.
16. T. Zhang and R. G. Barry, "The Sensitivity of Permafrost to Climate Change: Empirical Relations from Observations and Simulations," *Climatic Change*, vol. 52, no. 1–2, pp. 161–182, 2002.

APPENDIX

PYTHON AND GOOGLE EARTH ENGINE CODE

A. PYTHON SCRIPTS

A.1 Permafrost Mapping and Active Layer Thickness (ALT) Calculation

This script calculates TTOP, MAGT, ALT, and permafrost probability from input raster datasets (e.g., LST, NDVI, slope, DEM, and soil layers).

```

import rasterio
import numpy as np
import os
from rasterio.enums import Resampling
import matplotlib.pyplot as plt
from skimage.transform import resize

# Define helper to read and resample rasters to reference shape and
# transform
def read_and_resample(path, ref_profile):
    with rasterio.open(path) as src:
        data = src.read(
            1,
            out_shape=(ref_profile['height'], ref_profile['width']),
            resampling=Resampling.bilinear
        )
    return data

# Load reference raster for shape and profile
with rasterio.open('DEM_WesternHimalayas.tif') as ref:
    ref_data = ref.read(1)
    profile = ref.profile
    ref_shape = ref_data.shape

# Load and resample other rasters to match reference
lst = read_and_resample('MODIS_LST_WesternHimalayas.tif', profile)
ndvi = read_and_resample('NDVI_WesternHimalayas.tif', profile)
dem = ref_data # already loaded
slope = read_and_resample('Slope_WesternHimalayas.tif', profile)
aspect = read_and_resample('Aspect_WesternHimalayas.tif', profile)
nysi = read_and_resample('NDSI_WesternHimalayas.tif', profile)

```

```

bulk_density = read_and_resample('BULK_DENSITY.tif', profile)
sand = read_and_resample('SAND.tif', profile)
silt = read_and_resample('SILT.tif', profile)
clay = read_and_resample('CLAY.tif', profile)
coarse_frag = read_and_resample('COARSE_FRAGMENT.tif', profile)

# Fix FDD and TDD shapes by resizing if needed
with rasterio.open('Corrected_FDD_30m.tif') as src:
    raw_fdd = src.read(1)
    if raw_fdd.shape != ref_shape:
        raw_fdd = resize(raw_fdd, ref_shape, order=1,
preserve_range=True, anti_aliasing=False).astype(np.float32)
    fdd = np.nan_to_num(raw_fdd, nan=0.0, posinf=0.0, neginf=0.0)
    fdd[fdd < 0] = 0
    fdd = np.clip(fdd, 0, 5000)

with rasterio.open('Corrected_TDD_30m.tif') as src:
    raw_tdd = src.read(1)
    if raw_tdd.shape != ref_shape:
        raw_tdd = resize(raw_tdd, ref_shape, order=1,
preserve_range=True, anti_aliasing=False).astype(np.float32)
    tdd = np.nan_to_num(raw_tdd, nan=0.0, posinf=0.0, neginf=0.0)
    tdd[tdd < 0] = 0
    tdd = np.clip(tdd, 0, 5000)

# ---- Step 2: Estimate Thermal Conductivity Coefficients Based on
Soil Texture ----
Kf = 1.5 + 0.5 * (bulk_density / 1.6) + 0.01 * clay
Kt = 0.5 + 0.3 * (bulk_density / 1.6) + 0.005 * clay
Kf = np.clip(Kf, 0.5, 2.5)
Kt = np.clip(Kt, 0.2, 1.5)

# ---- Step 3: Estimate n-factors using NDVI and NDSI ----
nf = np.where(ndvi > 0.2, 0.7, 0.5)
nt = np.where(ndsi > 0.3, 0.6, 0.9)

# ---- Step 4: Approximate MAAT from LST (proxy) ----
MAAT = lst - 273.15

# ---- Step 5: Compute TTOP ----
TTOP = MAAT * nf - nt * (Kt / Kf)

# ---- Step 6: Compute Active Layer Thickness (ALT) ----
Lf = 334000
rho = bulk_density * 1000
k = 0.5 * (Kf + Kt)

print("--- Input Checks for ALT Calculation ---")
print("FDD: min=", np.min(fdd), " max=", np.max(fdd), " mean=",
np.mean(fdd))
print("rho: min=", np.min(rho), " max=", np.max(rho), " mean=",

```

```

np.mean(rho))
print("k: min=", np.min(k), " max=", np.max(k), " mean=",
      np.mean(k))

with np.errstate(divide='ignore', invalid='ignore'):
    ALT = np.sqrt((2 * k * fdd) / (Lf * rho))
ALT = np.nan_to_num(ALT, nan=0.0, posinf=0.0, neginf=0.0)
ALT = np.clip(ALT, 0, 5)

# ---- Step 7: Classify High Confidence Permafrost Zones Based on
ALT ----
permafrost_zone = np.where(ALT < 1.5, 1, 0)

# ---- Step 8: Combine MAGT + TTOP + ALT for Probability Score ----
dem_norm = (dem - np.min(dem)) / (np.max(dem) - np.min(dem))
slope_norm = (slope - np.min(slope)) / (np.max(slope) -
np.min(slope))
alpha = -1.5
beta = -2.2
delta = -0.5
epsilon = -0.2
C = 5.0

MAGT = alpha * lst + beta * ndvi + delta * slope_norm + epsilon *
dem_norm + C
MAGT = np.clip(MAGT, -20, 20)

TTOP_norm = (TTOP - np.nanmin(TTOP)) / (np.nanmax(TTOP) -
np.nanmin(TTOP))
MAGT_norm = (MAGT - np.nanmin(MAGT)) / (np.nanmax(MAGT) -
np.nanmin(MAGT))
ALT_inv = 1 - (ALT / 5.0)

permafrost_prob = (TTOP_norm + MAGT_norm + ALT_inv) / 3.0
permafrost_prob = np.clip(permafrost_prob, 0, 1)

print("ALT stats - min:", np.min(ALT), "max:", np.max(ALT), "mean:",
      np.mean(ALT))
print("Permafrost pixel count (ALT < 1.5m):", np.sum(permafrost_zone
== 1))

# ---- Downsample for Visualization Only ----
downsample = 10
ALT_vis = ALT[::downsample, ::downsample]
zone_vis = permafrost_zone[::downsample, ::downsample]
prob_vis = permafrost_prob[::downsample, ::downsample]

plt.figure()
plt.imshow(ALT_vis, cmap='magma')
plt.colorbar()
plt.title("Active Layer Thickness (ALT) [m]")
plt.show()

```

```

plt.figure()
plt.imshow(zone_vis, cmap='gray')
plt.colorbar()
plt.title("High Confidence Permafrost Map (ALT < 1.5m)")
plt.show()

plt.figure()
plt.imshow(prob_vis, cmap='plasma')
plt.colorbar()
plt.title("Permafrost Probability Map (Combined TTOP, MAGT, ALT)")
plt.show()

profile.update(dtype=rasterio.float32)
with rasterio.open('ALT.tif', 'w', **profile) as dst:
    dst.write(ALT.astype(np.float32), 1)

with rasterio.open('Permafrost_Probability.tif', 'w', **profile) as dst:
    dst.write(permafrost_prob.astype(np.float32), 1)

profile.update(dtype=rasterio.uint8)
with rasterio.open('PermafrostZone_ALT_lt_1_5.tif', 'w', **profile) as dst:
    dst.write(permafrost_zone.astype(np.uint8), 1)

print("Exported ALT.tif, PermafrostZone_ALT_lt_1_5.tif, and
Permafrost_Probability.tif")

```

B. GOOGLE EARTH ENGINE (GEE) SCRIPTS

B.1 GEE Script for Permafrost Input Data Extraction

This script extracts MODIS LST, Sentinel NDVI/NDSI, and other datasets clipped to the Western Himalayas boundary for use in permafrost modeling.

```

// Google Earth Engine script to extract necessary datasets for
permafrost modeling
// Define the region of interest (Western Himalayas)
var roi = ee.Geometry.Rectangle([75.5, 36.5, 80.5, 32.5]);

// 1. DEM - SRTM 30m
var dem = ee.Image("USGS/SRTMGL1_003").clip(roi);
Map.addLayer(dem, {min: 3000, max: 6000}, "DEM");

// 2. Slope and Aspect
var getSlopeAspect = function(dem) {
  var terrain = ee.Terrain.products(dem);
  return terrain.select(["slope", "aspect"]);
}

```

```

};

var slopeAspect = getSlopeAspect(dem);
Map.addLayer(slopeAspect.select("slope"), {min: 0, max: 60},
"Slope");
Map.addLayer(slopeAspect.select("aspect"), {min: 0, max: 360},
"Aspect");

// 3. Land Surface Temperature - MODIS (MOD11A2)
var lst = ee.ImageCollection("MODIS/006/MOD11A2")
  .filterDate("2020-01-01", "2023-12-31")
  .filterBounds(roi)
  .select("LST_Day_1km")
  .mean()
  .multiply(0.02).subtract(273.15); // Scale and convert to Celsius
Map.addLayer(lst, {min: -20, max: 20, palette: ["blue", "white",
"red"]}, "MODIS LST");

// 4. NDVI - MODIS MOD13Q1
var ndvi = ee.ImageCollection("MODIS/006/MOD13Q1")
  .filterDate("2020-06-01", "2023-09-30")
  .filterBounds(roi)
  .select("NDVI")
  .max()
  .multiply(0.0001);
Map.addLayer(ndvi, {min: 0, max: 0.8, palette: ["brown", "yellow",
"green"]}, "NDVI");

// 5. NDSI - from Landsat 8 SR
var landsat = ee.ImageCollection("LANDSAT/LC08/C02/T1_L2")
  .filterDate("2020-01-01", "2023-12-31")
  .filterBounds(roi)
  .filter(ee.Filter.lt("CLOUD_COVER", 10))
  .map(function(image) {
    var ndsi = image.normalizedDifference(["SR_B3",
"SR_B6"]).rename("NDSI");
    return image.addBands(ndsi);
  });
var ndsi = landsat.select("NDSI").median();
Map.addLayer(ndsi, {min: 0, max: 1, palette: ["black", "cyan"]}, "NDSI");

// 6. PISR - Potential Solar Radiation from DEM (approximate proxy
using hillshade)
var hillshade = ee.Terrain.hillshade(dem);
Map.addLayer(hillshade, {}, "Hillshade (PISR Proxy)");

// Export images
Export.image.toDrive({
  image: dem,
  description: "DEM_WesternHimalayas",
  scale: 30,
  region: roi,
}

```

```

    maxPixels: 1e13
  });

Export.image.toDrive({
  image: slopeAspect.select("slope"),
  description: "Slope_WesternHimalayas",
  scale: 30,
  region: roi,
  maxPixels: 1e13
});

Export.image.toDrive({
  image: slopeAspect.select("aspect"),
  description: "Aspect_WesternHimalayas",
  scale: 30,
  region: roi,
  maxPixels: 1e13
});

Export.image.toDrive({
  image: lst,
  description: "MODIS_LST_WesternHimalayas",
  scale: 1000,
  region: roi,
  maxPixels: 1e13
});

Export.image.toDrive({
  image: ndvi,
  description: "NDVI_WesternHimalayas",
  scale: 250,
  region: roi,
  maxPixels: 1e13
});

Export.image.toDrive({
  image: ndsi,
  description: "NDSI_WesternHimalayas",
  scale: 30,
  region: roi,
  maxPixels: 1e13
});

```

B.2 GEE Script for ERA5-Land Frost and Thaw Degree Days (FDD & TDD) Calculation

This script calculates cumulative Freezing and Thawing Degree Days from ERA5-Land temperature data for thermal modeling.

```
// Define region (Western Himalayas - adjust as needed)
```

```

var region = ee.Geometry.Rectangle([75.5, 36.5, 80.5, 32.5]); //  

example coordinates  
  

// Load ERA5-Land daily data  

var era5 = ee.ImageCollection('ECMWF/ERA5_LAND/DAILY_AGGR')  

    .select('temperature_2m')  

    .filterDate('2020-01-01', '2025-01-01')  

    .filterBounds(region);  
  

// Convert to Celsius  

var era5C = era5.map(function(img) {  

    return img.subtract(273.15).copyProperties(img,  

    ["system:time_start"]);  
});  
  

// Compute FDD and TDD  

var fdd = era5C.map(function(img) {  

    var negTemp = img.lt(0).multiply(img.abs());  

    return negTemp.set('system:time_start',  

    img.get('system:time_start'));  
});  
  

var tdd = era5C.map(function(img) {  

    var posTemp = img.gt(0).multiply(img);  

    return posTemp.set('system:time_start',  

    img.get('system:time_start'));  
});  
  

// Reduce over time to get cumulative FDD and TDD  

var totalFDD = fdd.reduce(ee.Reducer.sum());  

var totalTDD = tdd.reduce(ee.Reducer.sum());  
  

// Display on map  

Map.centerObject(region, 6);  

Map.addLayer(totalFDD.clip(region), {min: 0, max: 1000, palette:  

['blue', 'white']}, 'FDD');  

Map.addLayer(totalTDD.clip(region), {min: 0, max: 2000, palette:  

['green', 'red']}, 'TDD');  
  

Export.image.toDrive({  

    image: totalFDD.clip(region),  

    description: 'FDD_2020_2025',  

    region: region,  

    scale: 1000,  

    crs: 'EPSG:4326',  

    maxPixels: 1e13
});

```